CHARACTERIZING CEREBRAL SMALL VESSEL DISEASE WITH A FOCUS ON CADASIL AS A GENETIC MODEL -AN MRI BASED APPROACH

PhD Thesis

Dr. Bence Barna Gunda

Semmelweis University
János Szentágothai School of Neurosciences

Supervisor: Dániel Bereczki MD, DSc

Consultant: Hugues Chabriat MD, PhD

Reviewers: László Oláh MD, PhD
Péter Barsi MD, PhD

Head of Examination Committee: László Tringer MD, DSc

Members of Examination Committee: Zoltán Benyó MD, DSc
Attila Valikovics MD, PhD

Budapest, 2012

Content

Abbreviations

ADC: apparent diffusion coefficient

ADEM: acute disseminated encephalomyelitis

CADASIL: Cerebral Autosomal Dominant Arteriopathy with Subcortical Infarcts and Leukoencephalopathy

CARASIL: Cerebral Autosomal Recessive Arteriopathy with Subcortical Infarcts and Leukoencephalopathy

cMB: cerebral microbleeds

CNS: central nervous system

CRV: Cerebroretinal vasculopathy

CSF: cerebrospinal fluid

CST: corticospinal tract

cSVD: cerebral small vessel disease

CT: computed tomography

DWI: diffusion weighted imaging

DTI: diffusion tensor imaging

FLAIR: fluid attenuation inversion recovery

HERNS: Hereditary endotheliopathy with retinopathy nephropathy and stroke

HG: histogram

HVR: Hereditary vascular retinopathy

LI: lacunar infarct

MA: migraine with aura

MELAS: mitochondrial myopathy, encephalopathy, lactic acidosis, and stroke

MD: mean diffusivity

MRI: magnetic resonance imaging

PADMAL: Pontine autosomal dominant microangiopathy and leukoencephalopathy

PML: progressive multifocal leukoencephalopathy

PRES: posterior reversible encephalopathy syndrome

PWI: perfusion weighted imaging

PXE: Pseudoxanthoma elasticum

ROI: region of interest

RVCL: Retinal vasculopathy with cerebral leukodystrophy

SSPE: Subacute sclerosing panencephalitis

VRS: Virchow-Robin spaces

WMH: white matter hyperintensities

1. Introduction

1.1. Cerebral small vessel disease

Cerebral small vessel disease (cSVD) is a spectrum of clinical and imaging abnormalities linked to the pathology of small penetrating arteries and arterioles in the brain irrigating subcortical structures [1]. Accumulating data suggest that cSVD is the most prevalent neurological disorder in the ageing society of the developed world [2, 3]. The prevalence of its seemingly asymptomatic manifestations –silent brain infarcts- increases with age from approximately 6-7% at 60 years to 28% at 80 years of age according to a recent review [4]. In another study lacunar infarcts were found in 23% of all subjects over 65 years, and in 43% of subjects over 80 years of age [5]. Its acute, symptomatic manifestations –lacunar strokes- account for approximately 20% of all ischemic strokes [6-8]. Thus improved management of cSVD based on better understanding of the disease is of great importance.

cSVD is characterised by the arteriolosclerosis and/or microatheromatosis of small calibre (50-500 μm) cerebral arterial vessels caused by various pathologies [1]. Its most common, sporadic, form is related to age and vascular risk factors including hypertension and diabetes in particular. Inherited forms are increasingly recognised with CADASIL (Cerebral Autosomal Dominant Arteriopathy with Subcortical Infarcts and Leukoencephalopathy) being the most prevalent genetic cSVD [9, 10]. Inflammatory, infective and immunologically mediated forms are usually part of systemic diseases of diverse origin characterised by central nervous system vasculitis [11]. Cerebral amyloid angiopathy (CAA) –a pathological hallmark of Alzheimer's disease- affects small vessels both cortically and subcortically and may also lead to ischemic changes, although it is particularly associated with recurrent lobar haemorrhages [11]. In this thesis I will only focus on the most common and well-studied age and vascular risk factor related form of cSVD and CADASIL.

cSVD predominantly affects perforating end-arteries branching usually perpendicularly from a large parent artery. These penetrating arteries irrigate the so called perforator areas including the basal ganglia and internal capsule (lenticulostriate arteries from the anterior cerebral artery (ACA) A1 segment and middle cerebral artery (MCA) M1 segment), the thalamus (thalamoperforators from the posterior cerebral artery (PCA) and posterior communicating artery (PCoA)), the pons (pontine perforators from the basilar artery

(BA)) and the hemispheric deep white matter -centrum semiovale (perforators from the cortical, leptomeningeal arteries) [12-15].

The pathological changes in cSVD lead to luminal narrowing, decreased autoregulation and vasoreactivity, and vessel wall damage in the cerebral microvessels resulting in their i. gradual stenosis, ii. sudden occlusion, iii. leakage or iv. rupture. As a consequence the subcortical brain tissue suffers from i.: diffuse chronic hypoperfusion and ischemia leading to the progressive disintegration of cerebral white matter [16]; ii.: acute localised ischemia resulting in lacunar infarcts [17]; iii.: blood extravasation seen as microbleeds [18]; and iv.: acute major haemorrhages [11, 19]. In an advanced state of the disease cerebral atrophy invariably occurs as a remote and/or diffuse consequence of vascular lesion burden [20]. The pathogenesis of cSVD manifestations is summarized in **Figure 1** [21].

The gradual ischemic tissue damage clinically manifests in i. progressive cognitive impairment mainly affecting executive function in the earliest stages and later leading to dementia of subcortical type; and ii. disability characterized by gait disturbances and other motor impairments, pseudobulbar palsies, urinary incontinence etc. Acute focal ischemia presents –if it involves main sensorimotor pathways- with the so-called lacunar syndromes. Cerebral microbleeds are usually asymptomatic and their clinical significance is yet to be determined.

Figure 1: *Pathogenesis of cSVD manifestations. Abbreviations can be found in the text.*

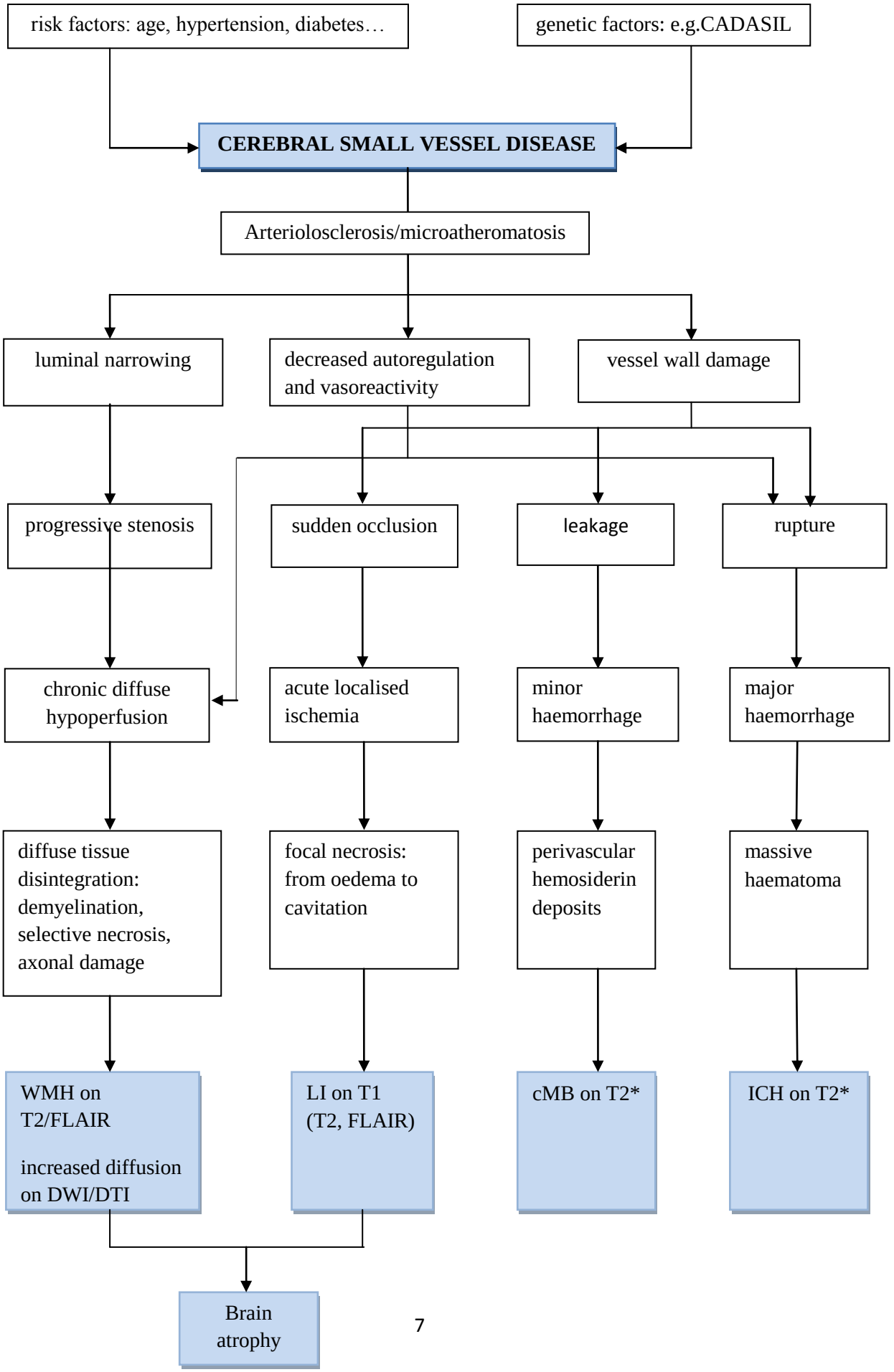

1.2. Magnetic resonance imaging of cerebral small vessel disease

Magnetic resonance imaging (MRI) is the most appropriate tool to assess cSVD. Since the cerebral microvasculature cannot be currently visualized in vivo, the consequent parenchymal lesions (lacunar infarcts, white matter lesions, microbleeds and atrophy) have been adopted as markers of cSVD [11]. Here I will summarize recent knowledge about the MRI characteristics of cSVD (without discussing the issue of major haemorrhages).

1.2.1. Lacunar infarcts

Definition

According to the "lacunar hypothesis" first proposed by Fisher small subcortical infarcts of a diameter less than 15 mm –called lacunar infarcts (LI)- result from the sudden occlusion of penetrating arteries due to cSVD in typical locations -the perforator areas (see above) [17]. Infarcts of this type have been linked to particular clinical syndromes with a relatively good prognosis called the lacunar syndromes, most frequent of which are the classical ones: pure motor stroke, pure sensory stroke, ataxic hemiparesis, dysarthria-clumsy hand syndrome and sensorimotor stroke. The concept of lacunar stroke that entered stroke classifications was based on postmortem and CT based studies both with considerable limitations. The pathological studies were limited by the low mortality of lacunar strokes and by the anatomical changes occurring in the chronic stage and/or during fixation. CT has a low sensitivity to detect small infarcts in certain locations (posterior fossa, cortex) and in the acute stage and cannot differentiate between fresh and old lesions. The advent of MRI and especially its newer techniques such as diffusion weighted imaging (DWI), perfusion weighted imaging (PWI) and diffusion tensor imaging (DTI) has slightly modified our understanding of LIs [21, 22].

Conventional MRI

Because of their small size visualizing LIs is much more problematic than that of larger territorial infarcts. Compared to CT conventional MRI sequences such as T1 weighted, T2 weighted imaging (T1/2WI) have a better spatial resolution, can image the posterior fossa without artifacts and have a better signal/noise ratio. LIs in the chronic stage appear as fluid

filled cavities: hypointensities (black holes) on T1WI and hyperintensities on T2WI isointense with CSF. More recent LIs can be seen as hyperintensities on T2WI corresponding to brain tissue with increased water content (oedema). The widely used T2 based fluid attenuation inversion recovery (FLAIR) sequence that nulls the hyperintense signal of free water (mainly CSF) has some advantages over the T2WI. FLAIR is more sensitive in the detection of small, recent infarcts in the proximity of CSF spaces like those in the cortex or next to the ventricles. It can better estimate the age of LIs, because the signal of bulk water in chronic infarcts (cavitations) is nulled as well, whereas the increased bound water content of acute infarcts (solid tissue) is hyperintense [23]. Acute lesions on FLAIR give a relatively stable high signal for several weeks as opposed to the fluctuations in intensity seen on T2W images [24, 25] (**Figure 2**). However very early ischaemia within the first few hours especially in the lacunar dimension cannot be seen on any of the conventional MR sequences, because the signal abnormality only appears 3-4 hours after symptom onset [26].

DWI

Acute stage imaging has been facilitated by the introduction of diffusion weighted imaging (DWI) that shows intracellular cytotoxic oedema resulting from critical cerebral ischaemia within the first few minutes after stroke onset [27]. The energy failure of brain cells, through the dysfunction of Na/K ATPase and consequent Na influx, results in the accumulation of intracellular bound water leading to a reduced diffusion of free water. This appears as marked hypointensity on the apparent diffusion coefficient (ADC) map which translates into high DWI signal [28-30]. In the case of cortical ischemia the reduced ADC returns to normal in 5-10 days (pseudo-normalisation) [25, 31], while it stays low for a considerably longer period in subcortical disease. Consequently the hyperintensity due to diffusion restriction is also visible for longer [32]. Later the ADC increases indicating vasogenic oedema and finally tissue disintegration/necrosis in the chronic stage [33]. However the lesion appearing hyperintense on DWI may remain visible further on as the developing T2 lesion is also seen as high signal (T2 shine through). Therefore DWI and ADC map images have to be interpreted together to judge the age of an ischaemic infarct [34, 35]. The sensitivity of this sequence within 6 hours of symptom onset is of 95% and its specificity is of practically 100% for territorial infarcts [36]. Although understandably less for small subcortical infarcts, it is still

the only reliable tool to visualise hyperacute LIs making it indispensable for acute phase therapy decisions (**Figure 2**).

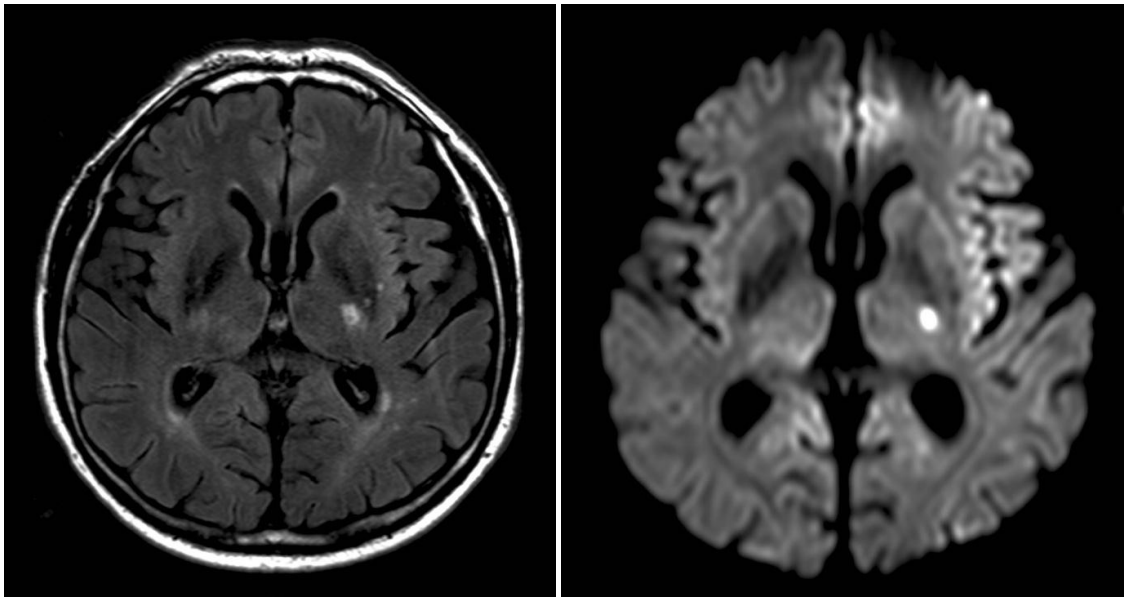

A B

Figure 2. *Subacute lacunar infarct in the posterior limb of the left internal capsule in a hypertensive patient on axial FLAIR (A) and DWI trace (B) image.*

DTI

A great proportion of LIs occur along the course of motor pathways whose affection well correlates with the severity of clinical symptoms and mainly determines prognosis. The extent of damage to these pathways can be judged by the MR diffusion tensor imaging (DTI) that is capable of visualizing white matter tracts [37]. This imaging method is based on the principle that cell membranes constrain the diffusion of water molecules which therefore diffuse longitudinally along axons in the white matter. By measuring diffusion from several directions the net orientation of axons in a voxel of white matter can be determined as a 3 dimensional vector –a „tensor". From these vectors virtual projections of fibres can be generated and displayed as maps of white matter anatomy e.g. in a colour-coded way where different colours stand for different directions, and colour brightness for the degree of anisotropy (colour-coded directional image) [38, 39]. Fiber tracking is a further development that enables examiners to visualize fibers passing through a certain region of interest (ROI) or

linking two ROIs thus delineating functional systems such as the corticospinal tract (CST). This method has been used to specifically localize small infarcts with regard to the functional pathway of the CST with good topographical accuracy [40-42] . Nevertheless, only a limited number of such tractography studies have been published to date, and few techniques have been assessed for their ability to track through lesions which disrupt tracts.

Size criterion

The size of LIs according to the classical definition is less than 15 mm –a rather arbitrary criterion based on early autopsy studies representing a healed, chronic state [17]. Since then we know that LIs in the acute stage can be significantly larger later undergoing shrinkage by about half their original size [43]. Furthermore surprisingly large infarcts can be caused by single perforator occlusion due to anatomic variations of the branching pattern of the lenticulostriate arteries. More or even all of the penetrating arteries may arise from one common stem [14, 44]. Therefore the size criterion for LIs can lead to stroke type misclassification and should be reconsidered [45].

Differentiation of underlying mechanisms

Apart from cSVD small subcortical infarcts may be caused by emboli of arterial or cardiac origin or critical hypoperfusion in watershed areas due to stenosing large artery disease (LAD). As determining stroke subtype is crucial for further management it is important to make an early etiological diagnosis. Acute lesion patterns on DWI help us to differentiate between the underlying pathomechanisms [46]. The co-existence of a small striatocapsular and one or more distal small cortical lesions points to an embolus originally stuck in the M1 segment obstructing the orifices of the lenticulostriate arteries and later on fragmented and washed further up into one or more small cortical branches of the MCA [47, 48]. This scenario is also possible in the posterior circulation -although much less frequently- with the picture of a small brainstem lesion together with a PCA territory thalamic or cortical infarct. Multiple small subcortical lesions in the same vascular territory are associated with LAD (arterio-arterial embolism), whereas those in different territories/bilaterally suggest a proximal embolic origin (heart or aortic arch) [49]. In the latter case it is not clear whether they result from repeated embolism or a single embolic shower [46].

It has also been proposed that multiple small infarcts may also be due to cSVD affecting several vessels contemporaneously [50]. As mentioned earlier subcortical lesions can remain hyperintense on DWI for much longer than cortical ones. Thus several lesions in diffferent vascular territories could arise contemporaneously (i.e. within a few weeks of each other) but not simultaneously and all appear hyperintense on DWI falsely raising the suspicion of an embolic origin. In addition the small perforators arising perpendicularly from large vessels seem hardly accessible for fast moving emboli from an anatomical point of view. Therefore the purely embolic origin of multiple small subcortical DWI lesions in multiple vascular territories remains debated.

Partial borderzone infarcts in the watershed of superficial and deep perforators of the MCA and/or ACA may also appear similar to LIs. They can be seen as a single small lesion or a chain of them (rosary-like pattern) in the centrum semiovale alongside and slightly above the lateral ventricle. The demonstration of ipsilateral carotid artery disease and consequent hypoperfusion shown by a perfusion deficit on perfusion weighted imaging (PWI) far exceeding the lesion area leads to diagnosis [51], [52].

Differentiation from other small cerebral lesions

LIs –especially when occurring without overt clinical symptoms, as incidential findings- may be difficult to distinguish from other hyperintense focal abnormalities on T2 weighted images. Studies correlating these lesions on in vivo and postmortem MR images with brain autopsy findings have identified the following pathologies: silent LIs, dilated Virchow-Robin spaces (VRS), foci of demyelination [53] due to incidental multiple sclerosis [54] or insufficient circulation [55] [56], gliosis, minute cysts and ventricular diverticuli [57, 58]. Distinction between an infarct, a focal gliosis and a plaque of demyelination is usually impossible on entirely imaging grounds, while the relationship of a diverticulum or cyst to the ventricles and their round shape are differential features [58].

VRSs are small perivascular spaces surrounding cerebral perforating arteries along their way through the parenchyma serving as drainage pathways for the cerebral interstitial fluid [59]. They are small (<1 mm) CSF isointense foci round shaped in cross section or linear in longitudinal section and run perpendicular to the brain surface [60-62]. Dilated VRSs that can resemble lacunes and appear as an irregular or ectatic focal expansion of the otherwise regular

and smooth VRSs [62]. They are still generally smaller than lacunes usually not exceeding 3 mm in diameter [63], whereas lacunes are larger and wedge shaped [61, 62]. Dilated VRSs have been associated with ageing [64], hypertension [65], widespread white matter lesions [66], sporadic cSVD [67] [63], CADASIL [68], reduced cognitive function [66], and vascular dementia [67, 69]. However their real clinical significance is a subject of controversy. It is generally accepted that dilated VRSs are related to brain shrinkage around perforating vessels thus representing brain atrophy [70]. In this perspective they can both be regarded as common ageing phenomenon or as a marker of various pathologies. The distinction between normal and pathologically dilated VRSs can be made by judging the appearance of the adjacent brain tissue and the clinical context [62].

Silent cerebral infarcts

With the increasing use of MRI and the improving image quality an increasing number of patients are found to harbour small cerebral infarcts without any apparent stroke-like symptoms. It has now become clear that LIs only cause clinically evident stroke if they hit main sensorimotor pathways or occur in deep, subcortical nuclei. However the majority of them fall outside of these strategic locations and thus remain silent. Studies have shown that in the general population the prevalence of silent infarcts is fivefold higher than that of stroke, and they can be present in more than one fourth of people over 60 years of age [71-74]. They have approximately the same risk factors as symptomatic lacunes with hypertension being the most important [73, 74]; and their presence more than doubles the risk of subsequent vascular events, cognitive impairment and dementia [4, 75]. The extent of asymptomatic small vessel disease at the time of index stroke has a significant prognostic value for all outcomes [43, 75]. These findings have led to a modified understanding of cerebrovascular disease according to which strokes and TIAs –i.e. overt clinical symptoms- are only the tip of the iceberg of cSVD manifestations [21, 22]. Silent infarcts are the underwater majority. It has not yet been evaluated though – and remains doubtful at present- whether the same diagnostic workup and risk factor management would be justifiable upon finding a silent infarct as for a clinical stroke. Although by definition silent infarcts lack clinically overt stroke symptoms they progressively lead to less evident cognitive dysfunction, general physical disability and depression. Therefore these infarcts should be referred to as "covert" rather than "silent" [4, 76].

1.2.2. White matter lesions

Definition

White matter lesions seen in elderly patients and those with arterial hypertension are usually bilateral and more or less symmetrical areas of increased signal on T2 and FLAIR images (hence the name: white matter hyperintensities, WMH) located in the hemispheric deep white matter and the pons (**Figure 3**). The term "leukoaraiosis" meaning rarefaction of white matter is a description from the CT era of the same phenomenon [77]. WMHs are generally regarded as a consequence of ischemic brain tissue disintegration due to cSVD. Pathological studies found varying degrees of tissue damage appearing as WMH: from selective loss of myelin, to loss of myelin, axons and oligodendroglia consistent with incomplete infarcts, to near complete infarcts with astrogliosis [78-81].

Differential diagnosis

Multifocal or diffuse white matter lesions resembling those caused by cSVD can be found in a wide range of central nervous system (CNS) pathologies. These are summarized in **Table 1**. Their differential diagnosis is based on the complex evaluation of patient history, clinical context, other diagnostic tests and some differences in MRI appearance. Some of these WMHs are also ischemic in origin such as those caused by hypoperfusion 1. in watershed areas due to large artery stenosis, or 2. in different vascular territories due to various types of CNS vasculitis. These latter can occur either as an isolated CNS affection (primary CNS vasculitis), or as part of a systemic disease (SLE, Sjörgen syndrome, Behcet disease, antiphospholipid syndrome, sarcoidosis etc.) Others are a consequence of multifocal demyelination in multiple sclerosis (MS) and its variants or in osmotic demyelination syndrome (formerly known as central pontine/extrapontine myelinolysis). As opposed to cSVD MS is characterized by ovoid-shaped lesions perpendicular to the ventricles (Dawson fingers), frequently found in the corpus callosum, some of which may enhance contrast material. Plaques may also be located in the optic nerves, cerebellum and spinal cord. WMH caused by transient vasogenic edema resulting from endothelial injury due to various complex conditions (preeclampsia/eclampsia, severe hypertension, allogenic bone marrow transplantation, organ transplantation, autoimmune diseases and high dose chemotherapy) has been termed as Posterior reversible encephalopathy syndrome (PRES). The typical pattern of

WMH in PRES resembles the watershed zones with a parietal and occipital (posterior) predominance. The subcortical white matter but also the cortex is involved to varying degrees and the lesions always regress [82]. White matter lesions of unclear nature can be seen in some infective diseases /postinfective conditions such as HIV, Lyme-disease or Syphilis related encephalopathies, Progressive multifocal leukoencephalopathy (PML), Subacute sclerosing panencephalitis (SSPE) or Acute disseminated encephalomyelitis (ADEM); and metabolic disorders like leukodystrophies, phenylketonuria and mitochondrial diseases (MELAS) [83, 84].

Table 1. *CNS pathologies causing multiple/diffuse white matter lesions. Abbreviations can be found in the text.*

Ischemia

- Watershed hypoperfusion in large artery stenosis
- Primary CNS vasculitis
- Secondary CNS vasculitis (SLE, Sjörgen syndrome, Behcet disease, antiphospholipid syndrome, sarcoidosis etc.)

Demyelination

- Multiple sclerosis and variants
- Osmotic demyelination syndrome

Endothelial dysfunction

- PRES

Unclear origin

- Infective/postinfective: HIV-, Lyme-, Syphilis- encephalopathy, PML, SSPE, ADEM
- Metabolic: leukodystrophies, phenylketonuria, MELAS

Evaluation with conventional MRI

The severity of white matter damage on T2 and FLAIR images can be assessed semiquantitatively by various visual rating scales (proposed by Fazekas[85], Schmidt [86], Scheltens [87], Wahlund [88] and others) that take into account the location, pattern and extension of WMH [89]. The mostly used Fazekas-scale which evaluates WMH in two distinct locations: periventricular and deep subcortical white matter is presented in **Table 2**. The mildest forms

are seen as smooth periventricular and punctuate deep WMH, whereas irregular periventricular, early confluent and confluent deep WMH represent an increasing severity of tissue damage. Furthermore the three dimensional extension of WMH can be quantified by volumetric evaluation [90, 91]. WMH volumetry is more reproducible and more sensitive for lesion progression than visual scales [92]. However the severity of white matter lesions as assessed by any of the above methods showed only moderate correlations with the clinical status represented by scores of disability and cognitive impairment [93-95].

Table 2. *Fazekas visual rating scale for WMH (0-6 points)* [85]

	periventricular	**deep subcortical**
0	absence	no or a single punctate lesion
1	„caps" or pencil-thin lining	multiple punctate lesions
2	smooth „halo"	beginning confluency of lesions
3	irregular PVH extending into deep WM	large confluent lesions

Evaluation with non-conventional MRI

The whole spectrum of microscopic brain tissue changes due to cSVD appears uniformly as WMH on conventional MR sequences. In order to obtain information on the degree of underlying tissue damage, non-conventional MRI techniques have been developed such as T1- and T2 relaxation time mapping, magnetisation transfer imaging (MTR) and diffusion tensor imaging (DTI) [96, 97]. This latter technique, that measures the degree and orientation of tissue water diffusivity, has been widely used in various cerebral diseases and conditions including cSVD [98]. As diffusivity partly depends on the density of cells in a given tissue volume (cell membranes and intracellular particles restrict water diffusion), the increase in diffusivity (as measured by a non-oriented derivate of the tensor, the mean diffusivity, MD) is proportional to the degree of ultrastructural tissue disintegration [99, 100]. Region of interest (ROI) based measurements detected increased MD inside but also outside of WMH, in the normal appearing white and subcortical grey matter [101, 102]. DTI can thus show tissue damage „invisible" for conventional MRI. In diffuse cerebral pathologies however -such as cSVD - a global, quantitative approach of whole brain diffusion histograms is more informative about the overall disease severity than a ROI analysis. Accordingly, MD histogram parameters have been reported to correlate more with clinical scores than WMH visual rating scales and volumetric data in cSVD both cross sectionally and longitudinally. Furthermore they were

more sensitive than clinical scales in detecting change over time [103-108]. In a study described further on in this thesis we obtained data indicating that the much simpler, quicker and widely available diffusion weighted imaging (DWI) derived apparent diffusion coefficient (ADC) can be used similarly to DTI derived MD to quantify brain damage due to cSVD (findings of Gunda et al. to be published) (**Figure 3 and 4**). Therefore these quantitative MRI techniques seem to be a promising tool in the quantified monitoring of cSVD and could possibly act as surrogate markers in future therapeutic trials.

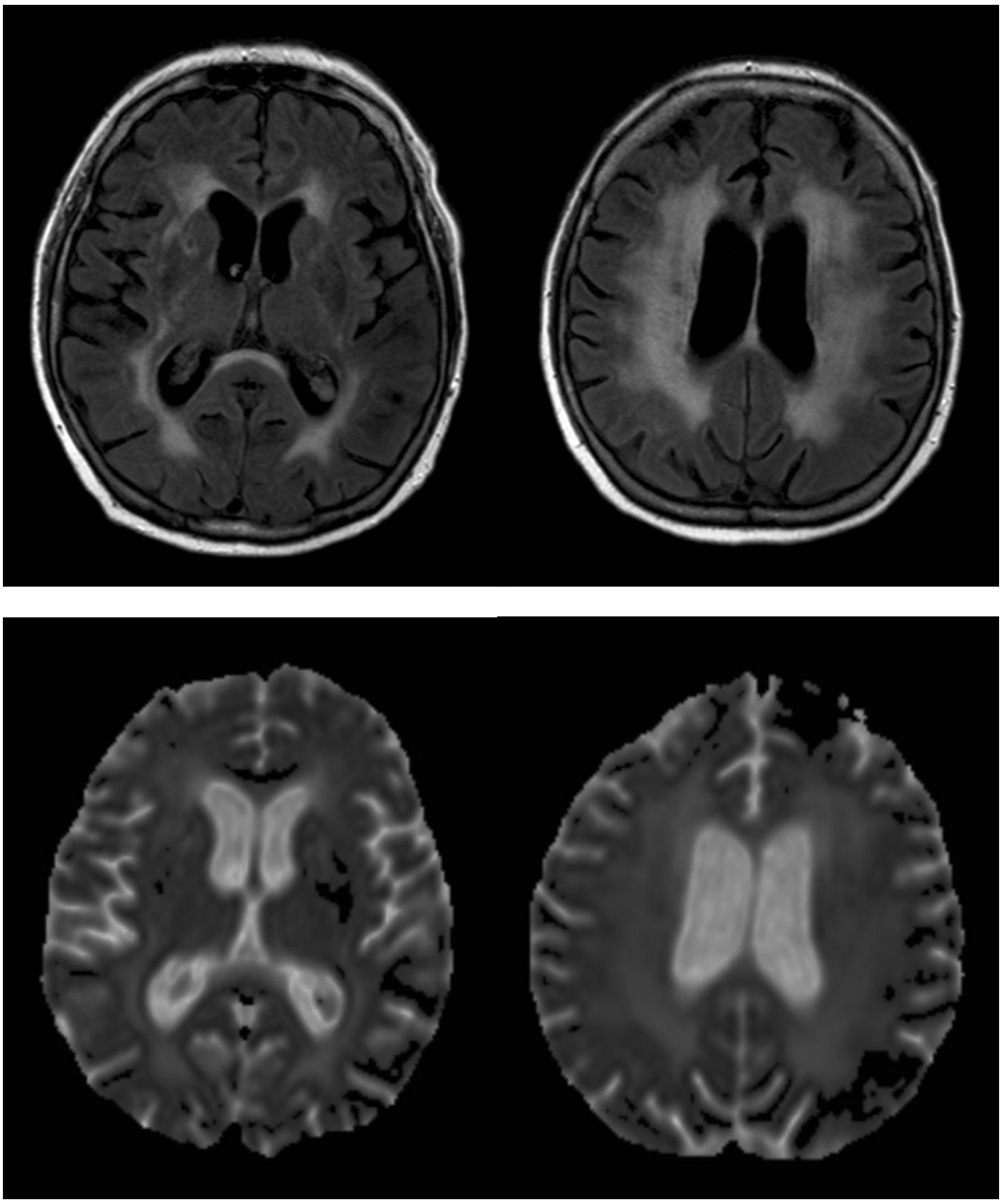

Figure 3. *Diffuse white matter lesions in a 70 year-old hypertensive patient on axial FLAIR image (upper row) and ADC map (lower row). Note the increased diffusion (ADC) corresponding to areas of WMH (FLAIR).*

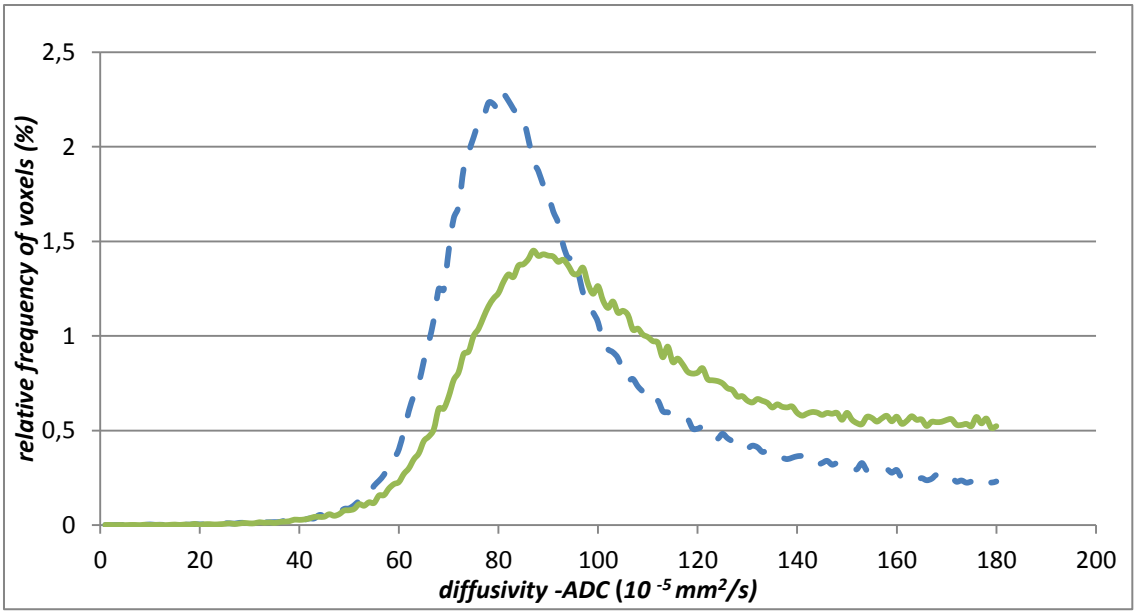

Figure 4. *ADC histogram of the patient on Figure 3 (green line) compared to a normal control (dashed blue line), diffusivity thresholded at 180x10 $^{-5}$ mm^2/s.*

1.2.3. Cerebral microbleeds

Definition

Gradient echo (or T2* weighted) imaging is a sequence highly sensitive of blood. With its increasing use the number of visible haemorrhagic brain lesions has grown considerably and even millimetre-sized bleedings in the parenchyma have become detectable. Cerebral microbleeds (cMB) appear as small (<5 mm), homogenous, rounded foci of low signal intensity on T2* images [109] (**Figure 5**). The signal loss is caused by hemosiderin –a paramagnetic blood degradation product that remains in macrophages for several years after haemorrhage indicating previous blood extravasation [110]. Thus the age of cMBs cannot be determined by MRI but the total haemorrhage burden can be assessed. Cerebral microbleeds appear larger on T2* images than the real tissue lesions due to the "blooming effect" of the MR signal [111]. The few studies relating cMBs on MRI to histopathological findings revealed focal hemosiderin deposits from the rupture of small vessels showing evidence of arteriolosclerosis or occasionally amyloid angiopathy clearly indicating an underlying small vessel pathology [18, 112].

Differential diagnosis

CMBs need to be distinguished from other causes of focal signal loss on T2* images. These include: flow voids of small arteries in cross-section that can be followed on consecutive/neighbouring slices; the usually symmetrical calcifications or iron deposits in the globi pallidi that appear hyperdense on CT; type IV cavernous malformations and capillary teleangiectasias; foci of hypointensity compatible with hemorrhagic shear injury in head trauma, and even artefacts of metallic materials released from mechanical heart valves [113, 114]. Etiological differentiation of signal loss is based on the location, number and distribution of lesions, associated imaging findings and patient history.

Epidemiology

CMBs have been found in various patient populations as well as healthy elderly. Their occurrence was the most frequent in patients with intracerebral haemorrhage (ICH) and lacunar infarcts (due to hereditary or sporadic cSVD), less so in ischemic stroke patients of other subtypes. The most comprehensive review on cMB published in 2007 pooled data from comparable studies and found the overall prevalence of cMBs to be 5% among healthy adults; 34% in ischemic stroke patients; and 60% in patients with ICH. The prevalence according to ischemic stroke subtype was 54% in lacunar-, 36% in atherothrombotic - and 19% in cardioembolic stroke. 38% of CADASIL patients had cMB. CMBs were more prevalent among patients with recurrent than first-ever stroke (44 vs 23% for ischemic and 83 vs 52% for haemorrhagic stroke) [115].

Clinical significance

CMBs were found to be associated with age, hypertension, other manifestations of cSVD (lacunar infarcts and WML), previous ischemic stroke and ICH, and an increased risk of recurrent lacunar infarct or ICH in those with lacunar infarct or ICH [115]. These findings further emphasize the common pathophysiological basis for cMB, LI, WML and ICH. Studies have shown that the anatomical distribution of ICHs is similar to that of cMBs in individual patients, but it is not the pre-existing cMBs that evolve into major haemorrhages [116]. Similarly several cases have been reported where patients with cMBs developed major haemorrhage after thrombolysis or antiplatelet therapy remote from the cMBs [117]. Thus cMBs can be considered as markers of a diffuse, bleeding-prone microangiopathy. This raised the important

question whether patients with cMB are at an increased risk of ICH when treated with antiplatelet, anticoagulant or thrombolytic agents. For the time being there is no sufficient evidence to give a definite answer (some studies reported an increased risk, others not, all of them underpowered to draw firm conclusions) [117-121]. However some stroke centres already incorporate cMBs in their treatment decisions.

In conclusion cMBs are markers of a haemorrhage-prone cSVD and predictors of recurrent vascular events (be it ischemic or haemorrhagic). At present they cannot be considered as a contraindication to antithrombotic or thrombolytic therapies, but may play a role in the individual stratification of haemorrhagic risk, and may be incorporated in the design of clinical trials of anticoagulation/antiaggregation drugs.

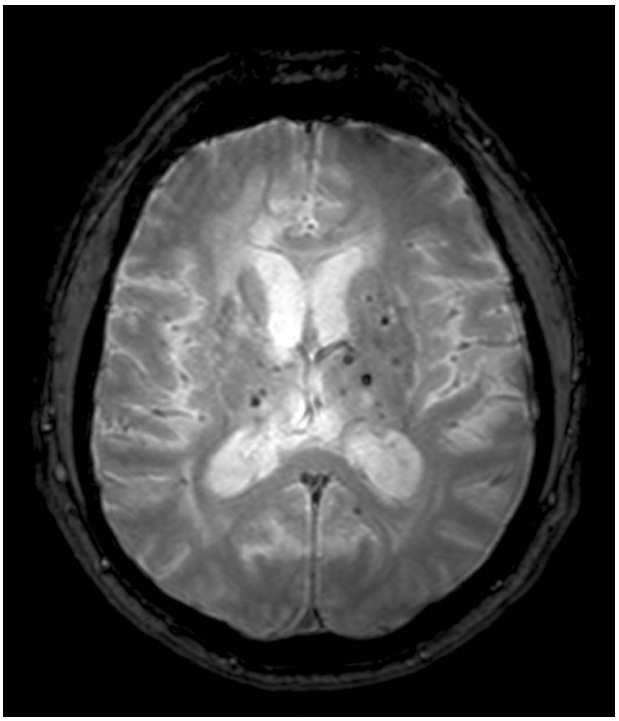

Figure 5. *Multiple cMBs in a 48 year-old hypertensive patient on axial T2* image.*

1.2.4. Brain atrophy

Brain atrophy is best evaluated on T1WI and appears as shrinkage of brain parenchyma with a reduction of cortical thickness and an increase of internal and external CSF spaces. It can be assessed by visually rating the degree of ventricular dilatation and

sulcal widening, by measuring the width of sulci or ventricles in a standard location, or by different three-dimensional volumetric methods that have now become the methods of choice.

Brain atrophy is a common phenomenon in normal ageing that increases progressively beyond the age of 65 years [122]. This process can be accelerated by numerous cerebral pathologies causing diffuse brain tissue loss such as degenerative diseases (like Alzheimer's disease and other primary dementias) [123], demyelinating diseases (MS) [124] and cerebrovascular disorders (**Figure 6**). In these latter conditions, the importance of brain atrophy has only recently been recognised. A number of imaging studies using quantitative brain volumetry demonstrated atrophy in both focal and diffuse cerebrovascular diseases [125-128]. Brain atrophy correlated strongly with the clinical status and cognitive scores, and proved to be a sensitive marker of disease progression in cSVD [106, 129, 130]. It is now widely accepted that purely subcortical cSVD can lead to cortical volume loss [130, 131]. How subcortical ischemic damage leads to cortical atrophy is not fully elucidated, but the diffuse and/or remote effect of lacunar lesions and tissue microstructural changes through Wallerian degeneration, secondary axonal loss due to deinervation and local or remote neuronal apoptosis are possible mechanisms [20, 125, 132, 133].

Brain atrophy is an aspecific finding and can be regarded as the final common pathway in the pathophysiology of various cerebral pathologies. As in degenerative diseases, atrophy is now recognized as a strong marker of disease progression in cSVD and thus could serve as a surrogate marker in future clinical trials similarly to whole brain diffusion histogram parameters [134].

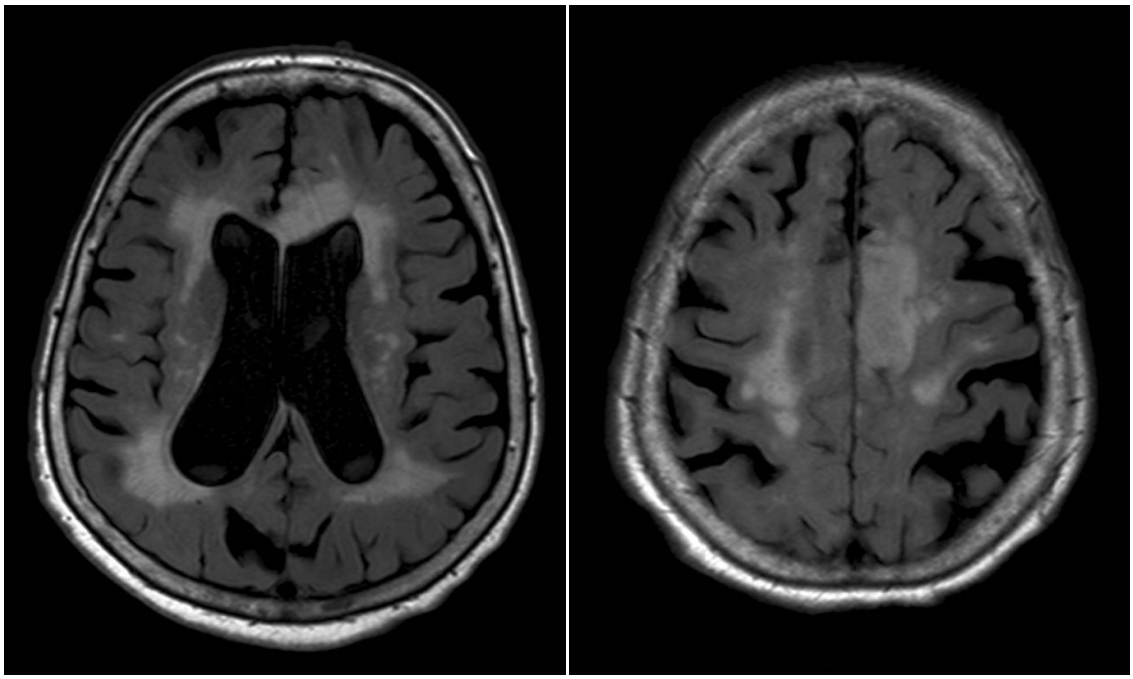

Figure 6. *Widespread WMH and diffuse brain atrophy in a 89 year-old hypertensive patient on axial FLAIR images.*

1.2.5. Summary

New and continuously developing MRI sequences and postprocessing techniques have greatly helped to explore and better understand cSVD. Diffusion MRI methods have proved to be particularly useful in: i. visualizing hyperacute LIs thus guiding acute phase therapy and etiologic diagnosis (DWI); ii. detecting ultrastructural changes even in otherwise normal appearing WM, and quantifying the global burden of tissue damage in cSVD (whole brain DTI/DWI histogram measures). Brain atrophy –a phenomenon previously considered to be related to cortical disease- is now recognised as a marker of cSVD based on studies using volumetric measures. In the future an increasing use of quantitative MRI techniques (diffusion histograms, volumetry) can be expected as they are more sensitive to the full spectrum of cSVD expressions, and could provide surrogate markers for disease progression in future therapeutic trials for patients with cSVD. The utility of different MRI sequences in cSVD is summarized in **Table 3**.

Table 3. *Utility of different MRI sequences in cSVD. Abbreviations can be found in the text.*

T1

- cavitated, chronic LIs appear hypointens („black hole")
- good for evaluation of brain atrophy and cortical thickness, volumetry as surrogate marker

T2

- subacute LIs appear hyperintens (fluctuating); good visualisation of VRS
- white matter damage appears as WMH; good for judging deep WMH

FLAIR

- (sub)acute LIs give more stable high signal; good for detection of periventricular LIs, differentiates acute (hyperintens) from chronic (hypointens) LIs
- white matter damage appears as WMH; good for judging both deep and periventricular WMH

T2*

- cMBs appear as small, hypointense foci, marker of bleeding-prone microangiopathy

DWI

- the only method to visualize (hyper)acute LIs that give high signal on DWI, low signal on ADC; acute lesion patterns guide differential diagnosis
- chronic LI gives low signal on DWI, ultrastructural tissue damage causes increased diffusivity (high signal on ADC map), whole brain ADC histogram as surrogate marker?

DTI

- localisation of LIs in relation to WM tracts (tractography)
- ultrastructural tissue damage causes increased diffusivity (high signal on MD map), whole brain MD histogram as surrogate marker

1.3. CADASIL and other hereditary small vessel diseases of the brain

1.3.1. CADASIL as a model disease

CADASIL (Cerebral Autosomal Dominant Arteriopathy with Subcortical Infarcts and Leukoencephalopathy) is a hereditary small vessel disease of the brain caused by mutations of the NOTCH 3 gene encoding a transmembrane receptor of vascular smooth muscle cells [9]. It has recently gained great interest in vascular neurology as the most common heritable cause of stroke and vascular dementia in adults. This autosomal dominant cSVD –unlike the sporadic, hypertensive form- appears already in adult midlife in the absence of vascular risk factors with ischemic episodes and progressive dementia. Its first clinical manifestation can be migraine with aura, and is often associated with psychiatric disturbances. The MRI changes may precede symptoms by more than a decade [135]. Apart from the well known and above discussed radiologic manifestations of cSVD in general, CADASIL has a unique feature: WMH symmetrically involving the temporal poles and the external capsule [136], see **Figure 7**. This characteristic pattern can be considered specific to the disease and is an important point in differential diagnosis [137-139] The special importance of this disease lies in the fact that CADASIL provides a pure genetic model for cSVD without the confounding factors of comorbidities and advanced age. Thus insights into CADASIL may help us better understand the more common sporadic forms as well.

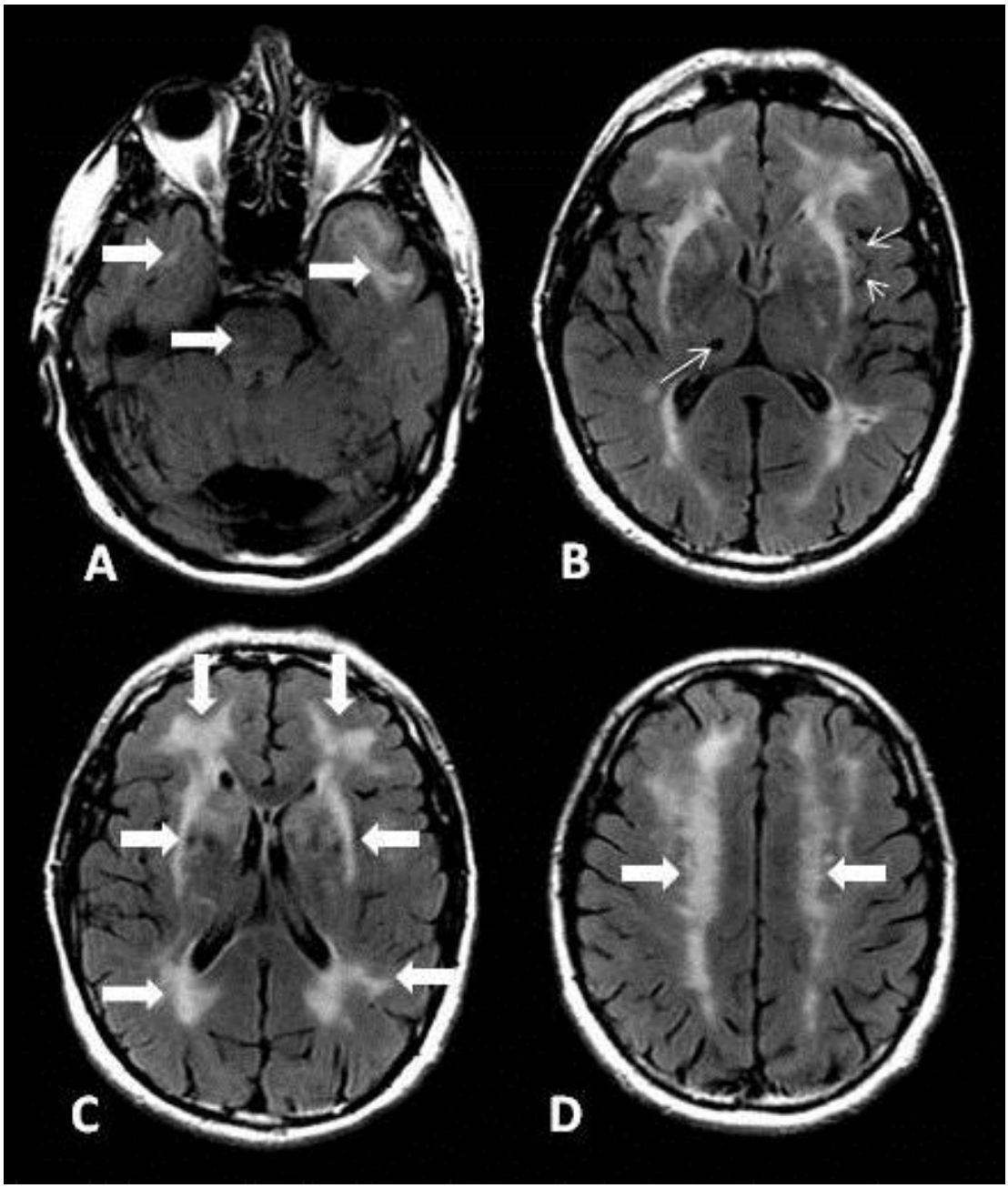

Figure 7. *Characteristic MR changes on axial FLAIR images in a 54 year old CADASIL patient:* ***A:*** *WMH in the pons and temporal poles (large arrows).* ***B:*** *Enlarged Virchow-Robin spaces (short arrows), lacunar infarct in right thalamus (long arrow), WMH of the external capsule.* ***C:*** *Frontal, periventricular and external capsule WMH (large arrows).* ***D:*** *WMH in corona radiata (large arrows).*

1.3.2. Other hereditary small vessel diseases of the brain

Besides CADASIL an increasing number of different hereditary small vessel diseases of the brain are being described (see **Table 4.**). To date the causal genes of four disorders with predominantly cerebral but also extracerebral involvement have been identified [140]. The autosomal recessive CARASIL (first described as Maeda syndrome in Japan [141, 142]) characterized by spinal deformities and alopecia is associated with mutations in the serine-protease HTRA 1 gene [143]. Syndromes affecting cerebral, retinal and renal vessels to a variable extent such as HERNS (Hereditary endotheliopathy with retinopathy nephropathy and stroke) [144], CRV (Cerebroretinal vasculopathy) [145] and HVR (Hereditary vascular retinopathy) [146] that were previously reported independently are now recognized as different phenotypes of the autosomal dominant Retinal vasculopathy with cerebral leukodystrophy (RVCL). It is caused by mutations in the TREX 1 gene encoding an exonuclease implied in the maintenance of vascular integrity [147]. Mutations in the COL4A1 gene encoding type IV collagen a1 chain, a component of basement membranes in various organs, have been found to be responsible for an autosomal dominant cSVD along with a whole spectrum of widely variable manifestations in the eyes, kidneys and muscles [148]. The most frequent phenotype in adults is characterized by subcortical intracerebral hemorrhages, diffuse cSVD and retinal arteriolar changes. HANAC syndrome (hereditary angiopathy with nephropathy, aneurysm and cramps) -a distinct phenotype- is dominated by systemic manifestations: hematuria, renal cysts, muscle cramps with elevated creatine-kinase and frequently bilateral aneurysms of the intracranial carotid artery [149]. Connective tissue changes are prominent in PXE (Pseudoxanthoma elasticum) associated with mutations in the ABCC 6 gene [150].

The exact genetic background of other cSVDs remains to be elucidated. These include Hereditary infantile hemiparesis already manifesting in early childhood [151] as well as other autosomal dominant hereditary cSVDs corresponding to the formal criteria of "Cerebral Autosomal Dominant Arteriopathy with Subcortical Infarcts and Leukoencephalopathy" without mutations in the NOTCH 3 gene. These conditions such as Hereditary small vessel disease of the brain [152], Hereditary multi-infarct dementia [153, 154], or SAE (Subcortical angiopathic encephalopathy also known as PADMAL i.e. Pontine autosomal dominant microangiopathy and leukoencephalopathy) [155, 156] could be termed as CADASIL type 2, 3, etc. in the future.

Table 4: *Hereditary small vessel diseases of the brain (Abbreviations can be found in the text)*

disease		**clinical features**	**genetics**
CADASIL		migraine with aura, stroke, apathy, dementia	NOTCH 3 on chromosome 19q12
CARASIL		stroke, dementia, kyphosis, lumbal disc herniation, bone deformities, alopecia	HTRA 1 on chromosome 10q26
RVCL	HERNS	stroke, renal disease, retinopathy, pseudotumors	TREX 1 on chromosome 3p21
	CRV	stroke, dementia, migraine, retinal capillary occlusions, blindness, pseudotumors, renal disease	
	HVR	retinal microangiopathia, blindness, migraine, Raynaud phenomenon	
COL4A1-related diseases		subcortical intracerebral hemorrhages, ischemic stroke, retinal arteriolar changes, hematuria, renal cysts, muscle cramps, intracranial aneurysms	COL4A1 on chromosome 13q34
PXE		skin and connective tissue abnormalities, stroke, blindness	ABCC 6 on chromosome 16p13
Hereditary infantile hemiparesis		infantile hemiparesis, retinal hemorrhages, migraine with aura	unknown
Hereditary small vessel disease of the brain		stroke, memory loss	unknown
Hereditary multi-infarct dementia		stroke, cerebellar symptoms, dementia	unknown
PADMAL (or SAE)		stroke, dysarthria, dementia	unknown

In the remaining part of this thesis I will present two studies performed in the world's largest cohort of CADASIL patients from the Lariboisière Hospital in Paris where the disease was identified, and the term CADASIL coined. The first one (Study 1) aimed to evaluate gender related differences in the clinical and MRI characteristics of the disease. It has recently been published [157]. The second study (Study 2) investigated the possible role of a DWI derived quantitative MRI method in disease monitoring.

2. Purpose

2.1. Effects of gender on the phenotype of CADASIL (Study 1)

In the general population, migraine, cerebrovascular diseases and vascular dementia differ in many aspects between men and women. The prevalence of migraine appears to be 3-4 times higher in women than in men.[158-161] In women, migraine is further influenced by the different stages of the reproductive life (menarche, pregnancy, menopause) or by the exposure to exogenous sex hormones such as contraception.[162] In contrast, the age-adjusted prevalence and incidence of stroke are respectively 30 and 40% higher in men than in women. [163] A similar trend for male sex is observed for the prevalence and incidence of vascular dementia.[164, 165] Accumulating evidence suggests that these differences may be related to female hormones that can both modify the excitability of the cortex [166, 167] and exert major neuroprotective effects.[168, 169]

CADASIL is considered as a model of "pure" subcortical ischemic vascular dementia and as a typical cause of secondary migraine with aura of vascular origin. Although some differences were previously reported between men and women in CADASIL [170], the exact role of gender in determining the phenotype of the disorder has not been specifically investigated.

In the present study, we evaluated the gender effect on the clinical and neuroimaging manifestations of CADASIL in a large cohort of CADASIL patients.

2.2. Whole brain ADC histogram in CADASIL (Study 2)

Unlike the conventional T1 and T2-weighted MR sequences, diffusion MRI is an imaging method that provides key information about the microstructural integrity of the cerebral tissue [99]. Alterations of diffusion tensor imaging (DTI) metrics (mean diffusivity – MD and fractional anisotropy –FA) were observed both inside and outside areas of increased signal on T2-weighted or FLAIR images in various white-matter disorders [102, 171-175]. In conditions with diffuse tissue lesions -such as multiple sclerosis, hypertension related cSVD, CADASIL or even in dementia or aging- a global, quantitative approach based on whole brain histograms of diffusion was found to be more informative about overall disease severity than using predefined regions of interest (ROI). Various DTI histogram parameters (mean value, median value, peak location, peak height, kurtosis, skewness) have been reported to correlate with clinical scores in these conditions both in cross-sectional and longitudinal studies. Moreover they were more sensitive than clinical scales in detecting change over time [96, 103, 106-108, 176-181]. In CADASIL, MD measured with DTI over the whole brain has been found to vary before any significant clinical change during follow up and to predict disease progression. DTI measures were then proposed as potential adjunct outcome measures in future therapeutic trials in CADASIL or in other cSVD [103-105, 129, 182]. The effects of sequences, scanners on DTI measures has been evaluated cross-sectionally in a small number of healthy volunteers [183, 184]

Measures of ADC over the whole brain from diffusion weighted imaging (DWI) commonly used in stroke patients without the use of much operator dependent post-processing may be an alternative method to obtain diffusion histograms. The main advantage of this approach would be the wide availability, simplicity and rapidity of the method suitable for everyday clinical use. The main drawback for longitudinal follow up studies with this method would be the variability related to the imaging-reimaging sessions, update of MRI sequences and changes of scanners.

In the present study, we aimed to evaluate whether ADC histograms obtained in a clinical setting would be suitable for follow up studies in cSVD as CADASIL. For this purpose, data from a large cohort of CADASIL patients with a follow up of 3 years were analyzed. The longitudinal evaluation of data is underway.

3. Methods

3.1. Subjects

A total of 313 CADASIL patients having a typical mutation of the Notch3 gene were included in Study 1. They were recruited from a large prospective cohort of patients investigated in Lariboisière Hospital in Paris (n=191) and the Ludwig Maximilians University's Neurology Clinic in Munich (n=122). The study was approved by an independent ethics committee at both centers; all patients gave a written informed consent to participate. 348 patients from the same cohort were included in Study 2.

3.2. Clinical evaluation

All subjects underwent a detailed neurological examination during the 2 hours preceding MRI examination, including a Mini-Mental State Examination (MMSE), Mattis Dementia Rating Scale and modified Rankin scale (mRS). Clinical and demographic data were collected including age, sex, cardiovascular risk factors (CVRF) including hypertension (defined as diagnosis of hypertension or taking antihypertensive drugs), diabetes (1997 World Health Organization criteria), hypercholesterolemia (diagnosis of hypercholesterolemia or taking lipid-lowering drugs), smoking habits and alcohol intake, history of migraine with aura (MA) (IHS diagnostic criteria), stroke, TIA, psychiatric symptoms including depression, apathy (based on Neuropsychiatric Inventory assessment applied in 132 patients only), seizures, gait and balance problems, hearing loss, urinary incontinence and presence of dementia (DSM IV criteria). Patients in Study 2 had follow-up examinations with an interval of 18 months over a period of 3 years.

3.3. MRI

The imaging protocol has already been detailed previously. [20] Briefly, MRI was performed on a 1.5-T system (Vision; Siemens [Munich] or Signa General Electric Medical Systems [Paris] with continuous updates [GE Signa 08, 09, Excite 11, 12, 14]). Three dimensional and millimetric T1-weighted MRI and FLAIR, T2*-weighted gradient echo, proton density and diffusion-weighted images of 5 mm thickness were obtained over the entire brain in axial planes. The parameters of diffusion-weighted imaging are as follows: Siemens: TR/TE 5100/137 ms, slice thickness 5 mm, interslice gap 1.5 mm, 128x128; b-value = 1000;

General Electric: TR/TE 8200/83 ms, slice thickness 5.5 mm, interslice gap 1.5 mm, 128x128; b value = 1000 s/mm^2.

To obtain ADC maps, diffusion-weighted imaging (DWI) scans were acquired in the X, Y, and Z directions and then averaged to make ADC measurements largely independent of the effects of anisotropic diffusion. Apparent diffusion coefficient values were then calculated for each voxel to generate ADC_{xyz} maps.

In a subset of patients Diffusion tensor imaging was also performed on GE Signa in 23 directions (B 0 and B = 700 in 23 directions; TR: 7500, TE: 98.8, EC: 1/1, bandwidth : 91Khz, thickness =5.5mm, 23 slices, matrix: 128*128, 1Nex). Eigen-vectors were obtained from all 23 directions for each voxel and eigen values were used for calculation of mean diffusivity (MD = Trace/23).

3.4. Image processing and analysis

Image processing and analysis for Study 1 have been previously reported by Viswanathan et al.[185] A dedicated software (Brainvisa) was used to determine the global brain volume from T1-weighted MR images after exclusion of CSF containing voxels in addition to the the volume of the intracranial cavity assessed on proton density images. Brain parenchymal fraction (BPF) was defined as the ratio of total brain tissue volume to the total intracranial cavity volume: BPF = (brain tissue volume/intracranial cavity volume) x 100. The volume of WMHs was obtained on FLAIR images, that of lacunar lesions on T1 scans. The total volume of WMH and that of lacunes were normalized to the intracranial cavity in each patient: normalized volume=(total volume / intracranial cavity volume) x 100. The number of microbleeds (MB) on T2* sequences was also recorded in each patient.

For Study 2 MD and ADC_{xyz} were first calculated over the whole volume of the brain. Histograms were obtained using a bin width equal to 0.1 x 10^{-4} mm^2/s and normalized over the number of voxels to correct for individual differences in brain size. The mean value, peak location and peak height of diffusion histograms were used for analysis.

Histograms derived from MD maps and obtained after CSF removal using a cutoff value of diffusion at 18 x 10^{-4} mm^2/s were used as the reference method for analysis of the parameters derived from ADC_{xyz} histograms.

To select the ADC_{xyz} histogram parameter best suited for clinical studies, correlations between parameters derived from MD histograms and those derived from ADC_{xyz} histograms were first analyzed before and after removal of voxels containing CSF using the cutoff value of 18 x 10^{-4} mm^2/s. Thereafter, correlations between parameters derived from MD and ADC_{xyz} histograms were evaluated before and after the manual removal of artifacts at the bone-air interface by an experienced neurologist; and before and after exclusion of the top and bottom 3 slices (containing the most artifacts and peripheral CSF).

The parameter derived from ADC_{xyz} histograms that best correlated with the reference method and was most independent from segmentation was chosen for subsequent analysis. A mixed-effects model was used to evaluate the effects of technical updates or change of scanners as seen in a clinical setting on diffusion parameters. Finally, the ability of parameters derived from ADCxyz histograms to predict the clinical course of CADASIL during the follow-up study was analyzed taking into account these potential limitations.

3.5. Statistical methods

In order to investigate the relationship between clinical manifestations, cognitive scores and MRI parameters between men and women in Study 1, we used the Student's t tests or Wilcoxon tests for categorical variables and ANCOVA for continuous variables. The comparison between men and women was performed after adjustments for age, history of cardiovascular disease, hypertension, diabetes, and education level according to the parameter under investigation. Comparisons were also made between women and men over or under the median age of the population (which corresponds approximately to the usual age of menopause) to investigate a potential hormonal influence. P values ≤ 0.05 were considered statistically significant.

In Study 2 correlations between the different parameters were evaluated by linear regression analysis and Bland-Altmann plots using JMP 8 software. A mixed-effects model was used to assess the magnitude of MRI scanner effect in the adjusted analysis of DWI parameters and clinical scores.

4. Results

4.1. Gender related differences

The clinical and MRI data from 313 patients (172 women and 141 men) whose mean age was 51 ± 11.4 years (women: 50.4 ± 12.2 years ; men = 51.8 ± 10.3 years) were analyzed. No significant difference was detected for the main cardiovascular risk factors (hypertension (22.6 in men vs 19.8% in women), diabetes (3.1 vs 1.5%), hypercholesterolemia (40.3 vs 43.0%), current smoking (25.2 vs 19.4%) and for any cardiovascular risk factor (79.7 vs 87.2%), with the exception of alcohol consumption (men: 79.1%;women: 49.7%, $p<0.001$).

The frequency of the main clinical manifestations of the disorder according to gender are presented in **Table 5**. The prevalence of MA was higher in women than in men. This female predominance was significant only in subjects under 51 years of age. Conversely, stroke events were more prevalent in men. This difference was also significant only in subjects aged less than 51 years.

In contrast the prevalence of TIA, age at first stroke and number of stroke events did not differ according to gender. We found no significant difference between men and women in the prevalence of dementia, psychiatric symptoms including depression, seizures, gait and balance problems, hearing loss and urinary incontinence. In contrast, apathy was found to be twice more prevalent in the male group, a difference significant both before and after 51 years.

Table 5: *Main clinical manifestations according to gender*

A: Prevalence (%) in the entire cohort

	Women	**Men**	**P***
migraine with aura	**44.2**	**31.2**	**0.02**
stroke	**57.6**	**74.5**	**0.003**
TIAs	38.1	29.5	0.14
age at first stroke (year; mean, SD)	49.2 (10.5)	48.2 (9.9)	0.30
multiple stroke events (in stroke patients)	52.0	55.2	0,35
psychiatric symptoms	47.7	44.0	0.48
apathy	**26.1**	**57.1**	**0.0001**
dementia	10.5	15.6	0.20

*adjusted for age, history of cardiovascular disease, hypertension and diabetes where appropriate

B: Prevalence (%) in subgroups of patients according to age more or less than 51 years

	≤ 51 years			**> 51 years**		
	Women	**Men**	**P***	**Women**	**Men**	**P***
migraine with aura	**53.6**	**35.4**	**0.03**	35.2	27.6	0.30
TIA	33.3	23.9	0.36	40.6	33.9	0.44
stroke	**40.5**	**70.8**	**0.0002**	73.9	77.6	0.64
Age at first stroke (year; mean, SD)	39.1 (0.8)	39.2 (0.7)	0.91	55.2 (0.7)	54.0 (0.7)	0.17
psychiatric symptoms	40.8	41.5	0.90	54.6	46.1	0.28
apathy	**3.3**	**44.8**	**0.0002**	**43.6**	**67.7**	**0.04**
dementia	2.4	6.2	0.40	18.2	23.7	0.39

*adjusted for history of cardiovascular disease, hypertension and diabetes where appropriate

The characteristics of MA in the two groups are presented in **Table 6**. In women, MA started at an earlier age (under 30 years in the majority of migraineurs) than in men. More women than men experienced visual and aphasic auras. The prevalence of sensory and motor auras as well as the frequency of migraine episodes, duration of aura and of headache and presence of triggering factors did not differ according to gender.

Table 6: *Characteristics of migraine with aura according to gender*

	Women	**Men**	**P**
age onset of MA (%)			
<30 years	**63.2**	**34.1**	
30-40 years	**26.3**	**43.2**	**0.008**
>40 years	**10.5**	**22.7**	
Visual aura (%)	**94.7**	**79.6**	**0.01**
Sensory aura (%)	76.1	67.8	0.26
Aphasic aura (%)	**71.1**	**52.3**	**0.04**
Motor aura (%)	21.1	22.7	0.83
Triggering factors (%)	28.9	29.6	0.94
duration of aura			
< 20 min	26.3	34.1	
20-60 min	60.5	47.7	
1-4 h	6.6	11.4	0.67
> 4 h	1.3	2.3	
no data	5.3	4.6	
duration of headache during MA			
< 4 h	30.8	26.3	
4-24 h	43.1	42.1	
1-3 days	16.9	18.4	0.74
> 3 days	0	2.6	
no data	9.2	10.5	
frequency of MA attacks			
>1/month	26.3	15.9	
< 1 /month to 1/3months	15.8	34.1	0.12
<1 /3 months to 1/2 years	39.5	24.1	
<1/2 years	18.4	15.9	

The comparison of baseline clinical scores between women and men is summarized in **Table 7**. Men were found to be more disabled than women with higher Rankin and NIHSS scores. There was no significant difference in global scores of cognitive performances (MMSE, Mattis), but men did worse in Mattis initiation test mainly evaluating executive functions. These differences were significant only in subjects over 51 years of age.

Table 7: *Main clinical scores according to gender*

A: in the entire cohort

Scores (mean, SD)	**Women**	**Men**	**P***
Rankin	**0.91 (1.4)**	**1.24 (1.5)**	**0.02**
NIHSS	**0.82 (1.7)**	**1.70 (3.1)**	**0.002**
MMSE	25.6 (4.4)	25.5 (4.5)	0.76
Mattis DRS	132.5 (18.3)	130.3 (17.8)	0.25
Mattis initiation	**33.4 (6.4)**	**31.9 (7.3)**	**0.04**

*adjusted for age and education level

B: in subgroups of patients according to age more or less than 51 years

Scores (mean, SD)	**< 51 years**			**> 51 years**		
	Women	**Men**	**P***	**Women**	**Men**	**P***
Rankin	0.38 (0.17)	0.41 (0.18)	0.85	**1.35 (0.30)**	**2.01 (0.29)**	**0.009**
NIHSS	0.77 (0.41)	1.07 (0.45)	0.39	**1.1 (0.5)**	**2.4 (0.5)**	**0.004**
MMSE	27.9 (0.5)	28.0 (0.6)	0.91	24.8 (1.0)	24.2 (1.0)	0.51
Mattis DRS	138.2 (2.2)	137.2 (2.4)	0.57	129.9 (4.1)	125.6 (3.9)	0.21
Mattis initiation	35.3 (0.8)	34.5 (0.9)	0.23	**32.5 (1.5)**	**29.9 (1.5)**	**0.05**

*adjusted for education level

The comparison of MRI parameters according to gender is summarized in **Table 8**. The brain parenchymal fraction was significantly lower in men, suggesting higher brain

atrophy in men compared to women. This finding was observed independently of age stratification. The volume of lacunar infarcts was 50% larger in men than in women but this difference did not reach statistical significance although the mean difference was 75% in subjects younger than 51 years. In contrast, the volume of WMH and number of MB did not differ between men and women.

Table 8: *MRI parameters according to gender*

A: in the entire cohort

MRI parameters (mean, SD)	**Women**	**Men**	**P***
WMH volume	0.071 (0.05)	0.074 (0.05)	0.71
Lacunar volume	*$2.4x10^{-4}$ ($5x10^{-4}$)*	*$3.5x10^{-4}$ ($6x10^{-4}$)*	*0.08*
Number of microbleeds	3.01 (12.6)	3.48 (14.2)	0.78
BPF	**86.7 (5.9)**	**83.6 (6.7)**	**<0.0001**

*adjusted for age

B: in subgroups of patients according to age more or less than 51 years

MRI parameters (mean, SD)	**< 51 years**			**> 51 years**		
	Women	**Men**	**P**	**Women**	**Men**	**P**
WMH volume	0.050 (0.04)	0.052 (0.04)	0.76	0.091 (0.05)	0.099 (0.05)	0.40
Lacunar volume	$1.6x10^{-4}$ ($4 x10^{-4}$)	$2.8 x10^{-4}$ ($5 x10^{-4}$)	0.09	$3.3 x10^{-4}$ ($6 x10^{-4}$)	$4.2 x10^{-4}$ ($6 x10^{-4}$)	0.42
Number of microbleeds	0.79 (4.8)	0.81 (2.2)	0.96	5.53 (17.4)	5.97 (19.4)	0.89
BPF	**89.5 (4.3)**	**86.4 (5.3)**	**0.0003**	**83.7 (6.0)**	**81.0 (6.9)**	**0.01**

4.2. Diffusion histograms

280 patients who underwent both DTI and DWI imaging were included in the first comparative part of our second study. 249 patients had DWI images with correction of artefacts and all patients (348) had DWI images with removal of top-bottom slices. The multivariate analysis included all patients (348) in the cohort.

The mean, peak or height values of ADCxyz histograms were found to be strongly correlated with the corresponding value of MD histograms obtained with DTI. The correlation coefficients (R^2) obtained in regression analysis for the mean, peak and height values were 0.964; 0.795 and 0.982 respectively with data obtained after CSF suppression, 0.965;0.722 and 0.974 with data obtained without CSF suppression on the GE excite 11 scanner (see **Table 9**). These correlations were found to vary according to scanner update but were similarly tight with and without CSF suppression (see **Figure 8**). (after CSF suppression on GE signa 08: 0,951; 0,790; 0,916, signa 09: 0,875; 0,606; 0,769; without CSF suppression on GE signa 08: 0,978; 0,790; 0,945, signa 09: 0,773; 0,606; 0,781.)

Table 9: *Correlation coefficients for ADC/MD parameters*

	mean	**peak**	**height**
with CSF suppression	0,964	0,795	0,982
without CSF suppression	0,965	0,722	0,974

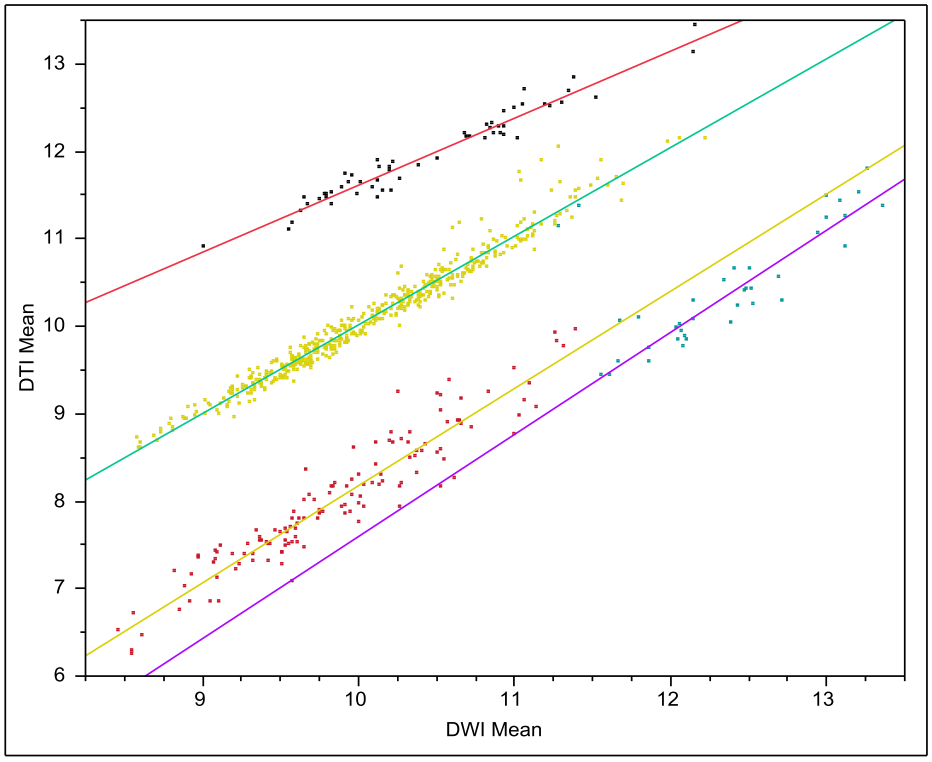

Figure 8: *Correlation of ADC-MD mean value on different scanners (GE updates) with CSF suppression*

The different parameters derived from ADC_{xyz}histograms obtained before and after CSF suppression were found strongly correlated. The correlation coefficients (R^2) for the mean, peak and height values were 0.742;1 and 0.958 respectively on all GE scanners together (see **Table 10** and **Figure 9**)(signa 08: 0.676; 1; 0.955 ; signa 09: 0.574; 1; 0.938; excite 11: 0.690; 1; 0.960), and 0.775; 1; 0.917 on the Siemens scanner. The results confirmed that the peak value of histogram was not influenced by diffusion values in CSF.

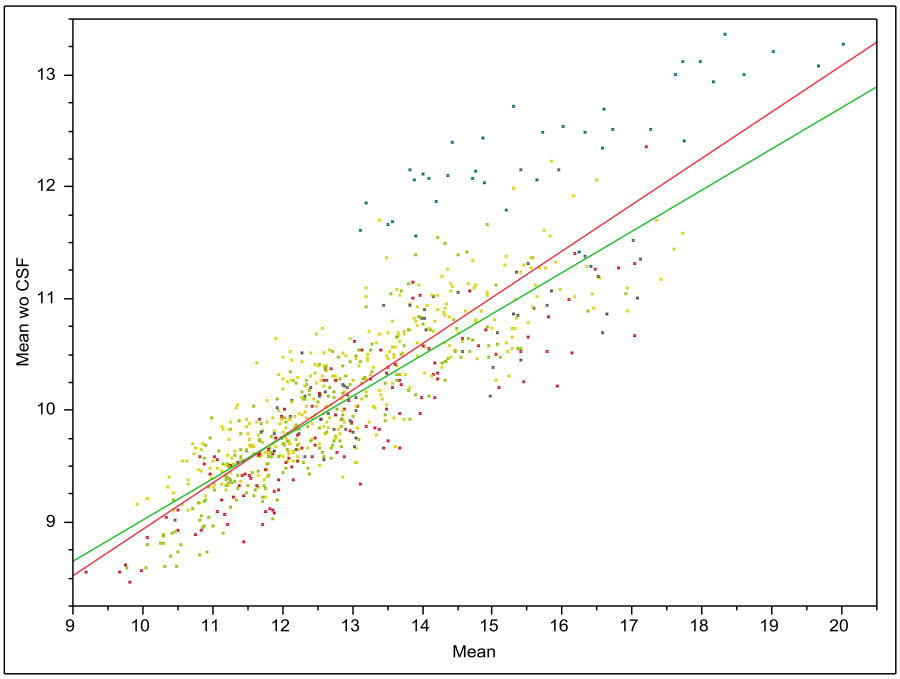
Mean wo CSF
Mean
9
10
11
12
13
14
15
16
17
18
19
20

A

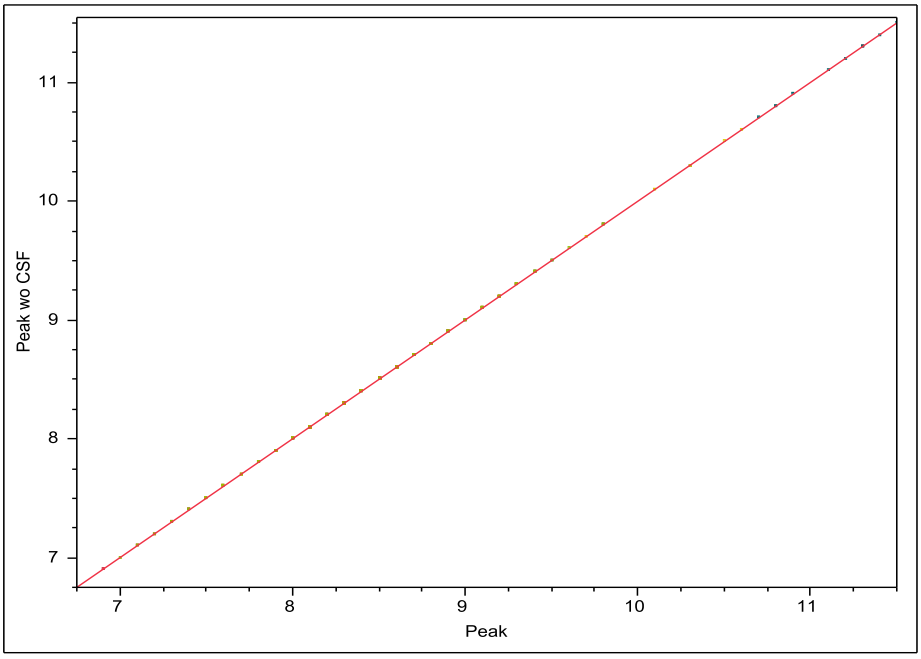
Peak wo CSF
Peak
7
8
9
10
11

B

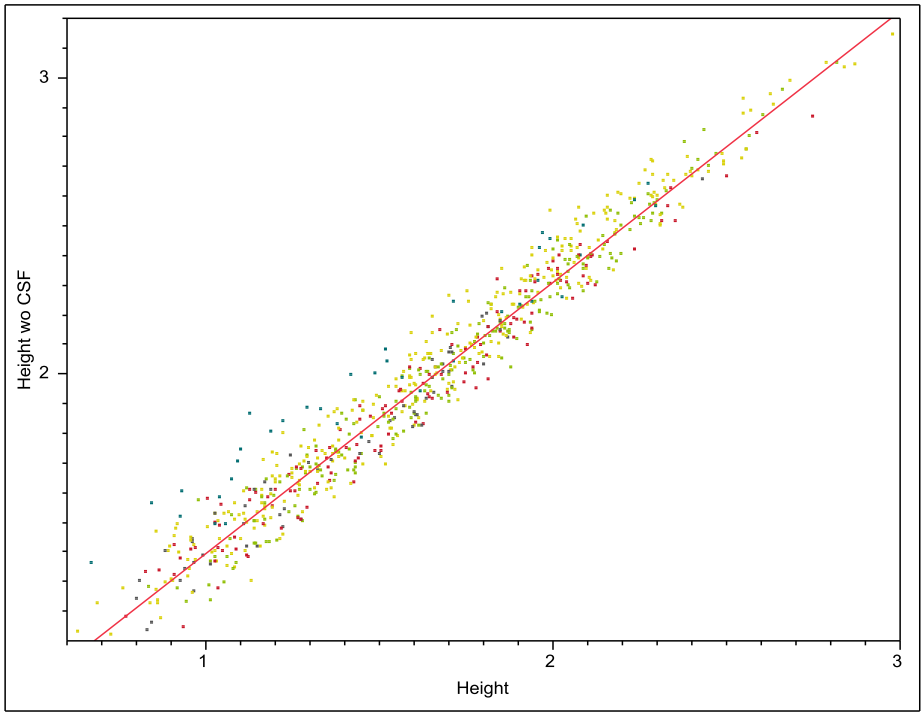

C

Figure 9: *Correlation of A mean, B peak and C height of ADC histogram with-without CSF suppression on all GE scanners*

The bland-Altmann plots showed that among the 3 parameters derived from diffusion histograms, the mean value derived from ADCxyz histograms after suppression of CSF had the tightest concordance with its referral measure obtained on DTI. The Bland-Altmann plot was narrow, horizontal and zero-centred for M, more dispersed but also zero-centred for P (showing the discrete nature of these data caused by the bins) and narrow but with a negative slope starting from zero for H. The plot for M without CSF suppression was similar to the original but wider and was significantly above zero. All plots were within the 0,5 limit. See **Figure 10**.

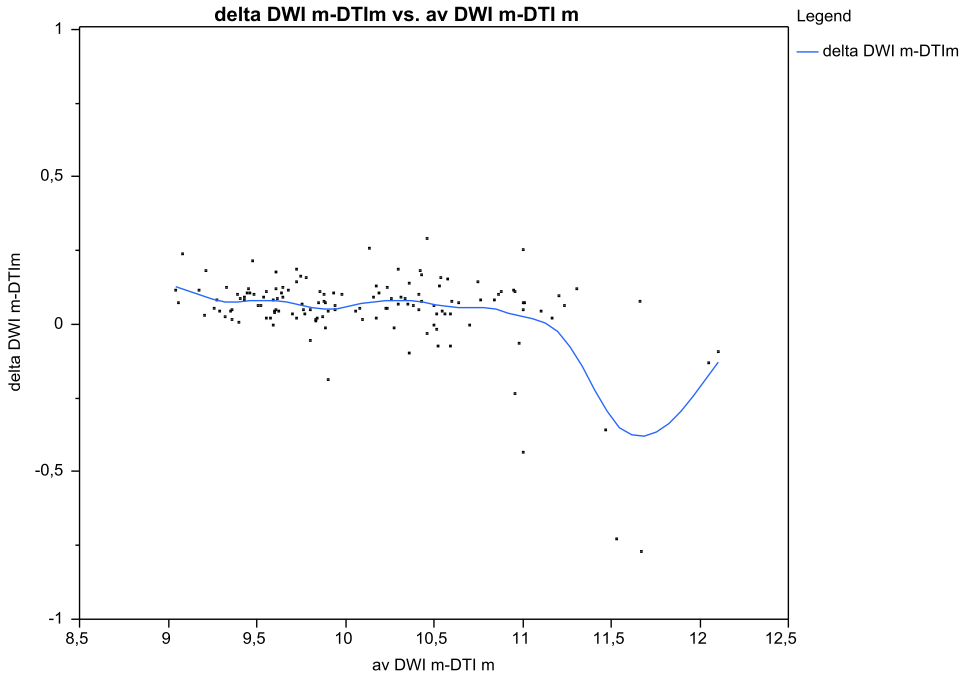
delta DWI m-DTIm vs. av DWI m-DTI m
Legend
delta DWI m-DTIm
delta DWI m-DTIm
av DWI m-DTI m
1
0,5
0
-0,5
-1
8,5
9
9,5
10
10,5
11
11,5
12
12,5

A

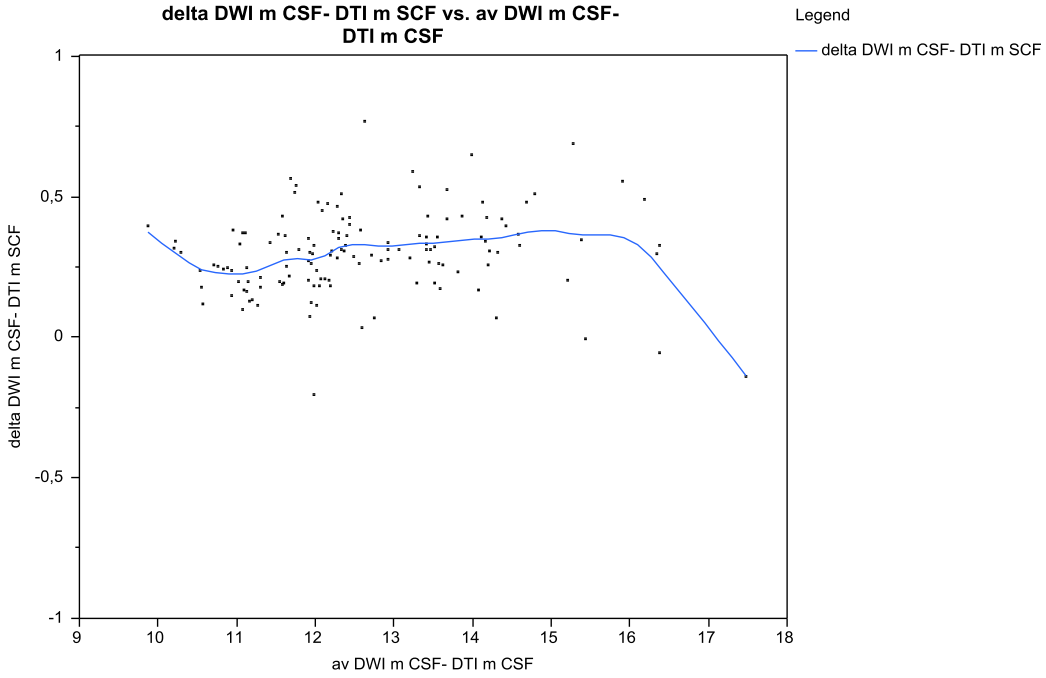
delta DWI m CSF- DTI m SCF vs. av DWI m CSF- DTI m CSF
Legend
delta DWI m CSF- DTI m SCF
delta DWI m CSF- DTI m SCF
av DWI m CSF- DTI m CSF
1
0,5
0
-0,5
-1
9
10
11
12
13
14
15
16
17
18

B

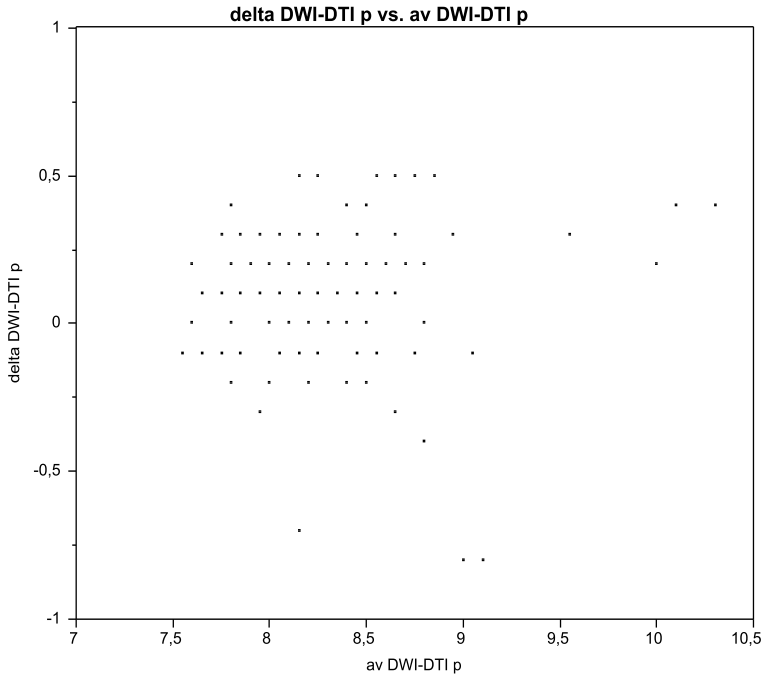

C

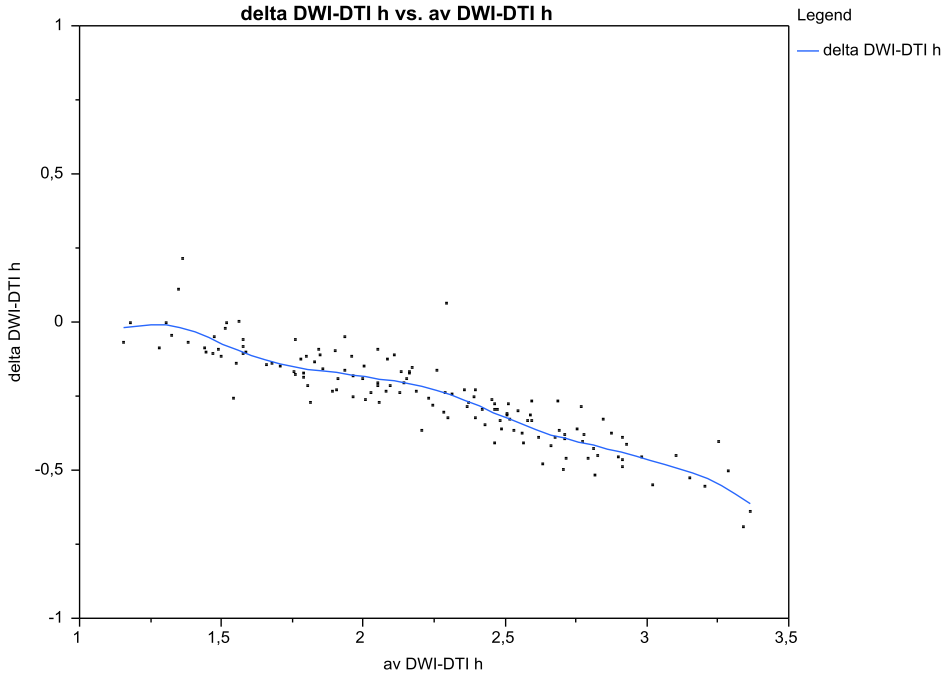

D

Figure 10: *Bland-Altmann plots for A mean value with CSF suppression, B mean value, C peak value, D height of ADC/MD hsitograms on the same scanner (GE Excite 11 new)*

The correlation of ADC_{xyz} parameters with and without removal of artifacts resulted in the following coefficients (R^2) for mean, peak and height values: 0.999; 0.996 and 0.997 on the GE and 0.998; 0.967; 0.997 on the Siemens scanner. The correlation coefficient (R^2) for parameters obtained with and without removal of the top-bottom 3 slices was 0.998; 0.986 and 0.997 on the GE and 0.993; 0.943 and 0.989 on the Siemens scanner (see **Table 10)**. The Bland-Altmann plots also showed very tight concordance for the mean value, less for P (see **Figure 11** and **12**).

Table 10: *Correlation coefficients for ADC parameters*

	mean	**peak**	**height**
with/without CSF suppression	0,742	1,0	0,958
with/without artefact removal	0,998	0,967	0,997
with/without top-bottom slices	0,993	0,943	0,989

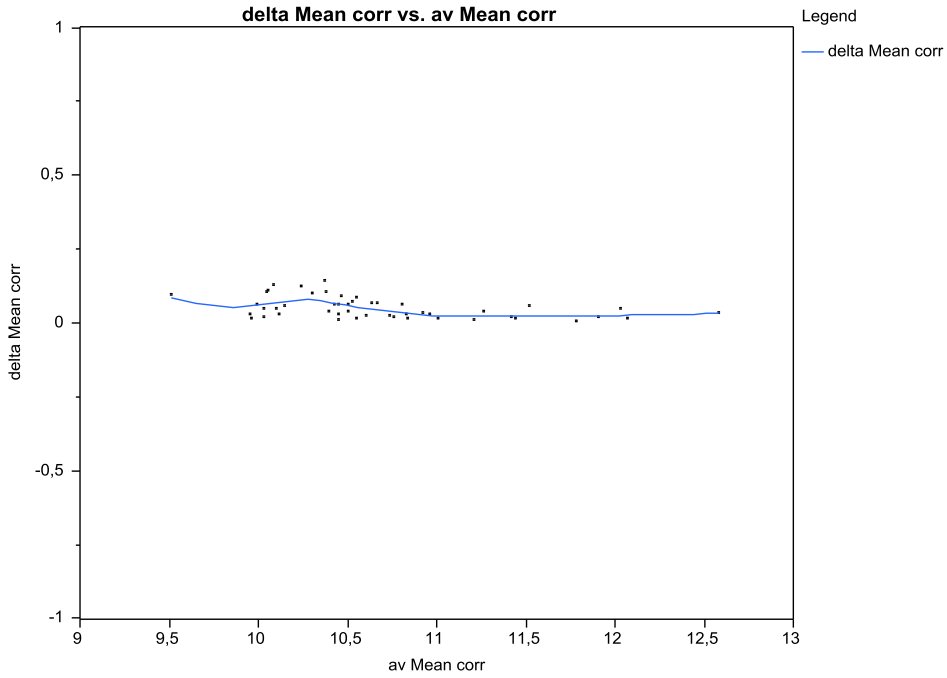

A

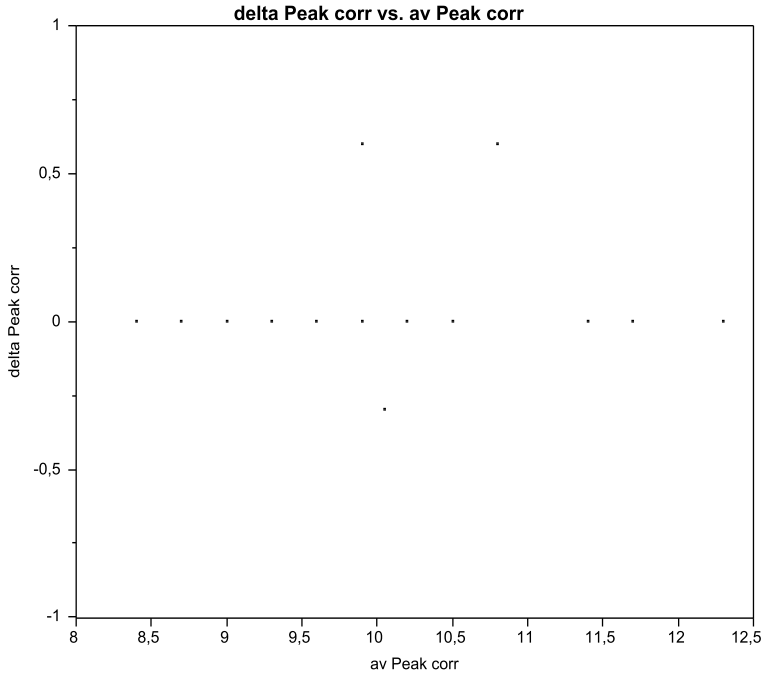

B

Figure 11: *Bland-Altmann plots for A mean and B peak value of ADC histograms with-without artefacts on the Siemens scanner*

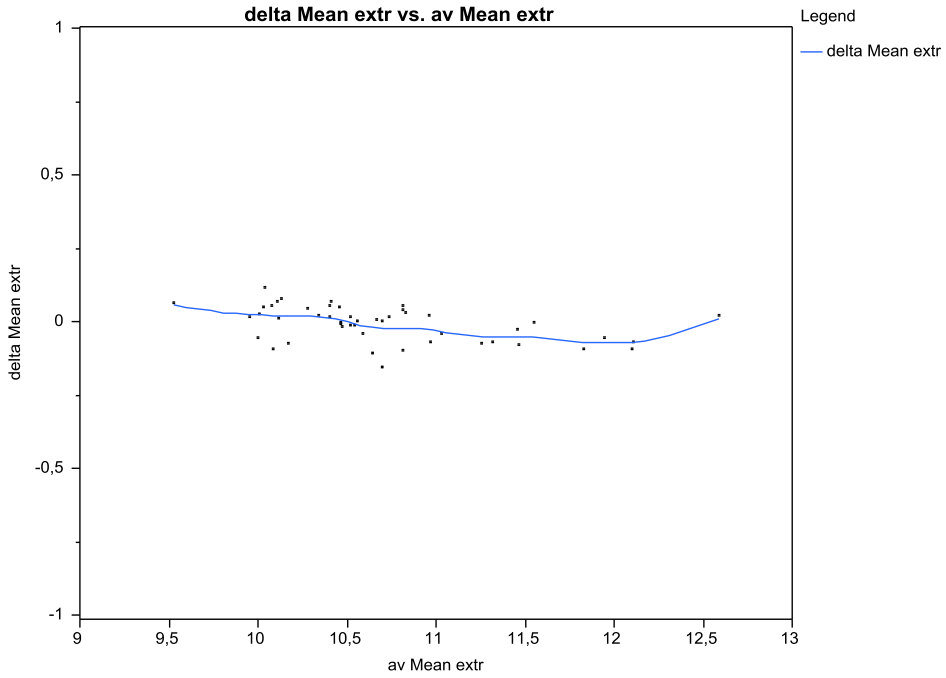

A

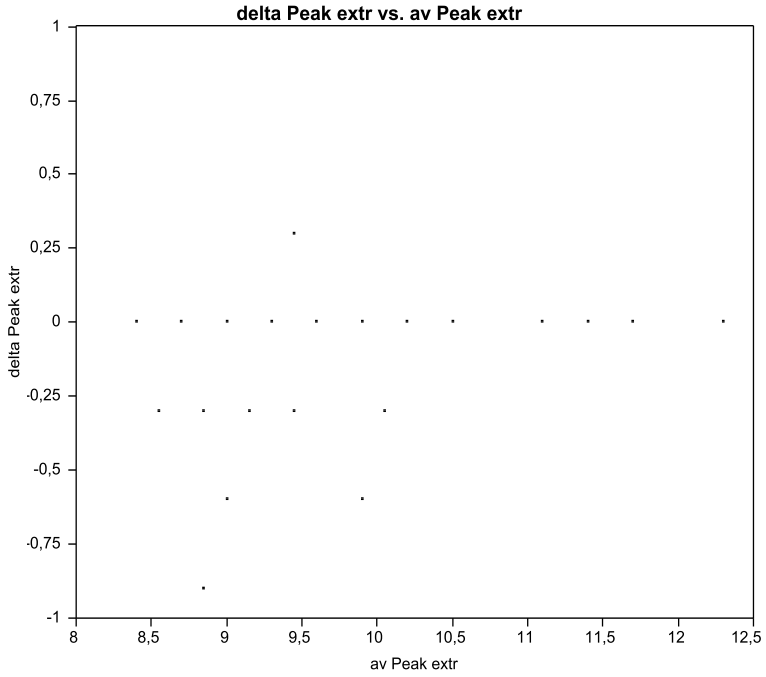

B

Figure 12: *Bland-Altmann plots for A mean and B peak value of ADC histograms with-without top-bottom 3 slices on the Siemens scanner*

The association between parameters derived from ADC_{xyz} histograms and clinical scores including the scanner effect is presented in **Table 11**. The results show that the standard deviation of the random scanner effect is larger than the regression coefficient of fixed effects of clinical scores, age or sex on mean value of ADCxyz histograms.

Table 11: *Magnitude of MRI scanner effect in the adjusted analysis of DWI parameters and clinical scores. Circles surface is proportional to the number of patients evaluated by each scanner, and their vertical position reflects the random MRI scanner effect. The gray shaded area represents the expected effect of 95% of scanners. For purpose of comparison, the (fixed) effects of clinical score differences given in the right margin are displayed by dashed lines.*

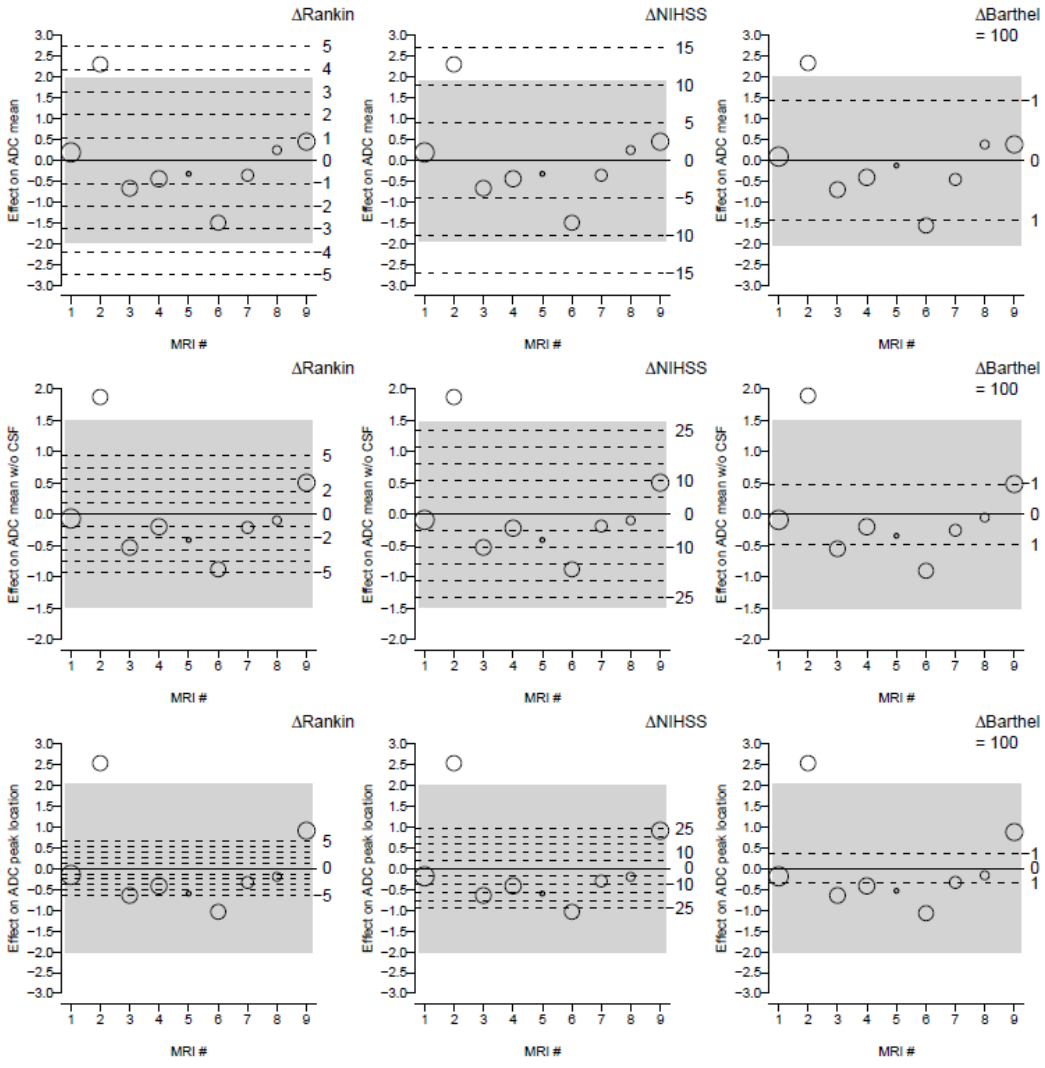

5. Discussion

5.1. Gender effects in CADASIL

There are two main findings in this large sample of CADASIL patients included in our first study: 1) before the usual age of menopause, MA appears to be more prevalent and stroke less prevalent in women than in men and this difference vanishes after the fifth decade, 2) in the whole population, men present with more apathy and higher degree of cerebral atrophy with a trend for a larger volume of subcortical infarcts. Moreover after the 5th decade men have more executive dysfunction and disability than women. The larger prevalence of MA in CADASIL women is in line with data obtained in the general population showing a nearly twofold excess of MA in women compared to men. [158-160, 186] MA has been associated with high levels of circulating estrogen in women.[187] In animal models, ovarian hormones were also previously shown to increase cortical excitability that promotes spreading depression (SD) most likely responsible for the aura symptoms in humans.[167, 188-191] Experimental data recently showed that the susceptibility to cortical spreading depression is actually increased in CADASIL transgenic mice.[192] In the present study, the differences in prevalence and presentation of aura symptoms according to gender suggest that the hormonal status may further modulate this susceptibility in CADASIL patients.

The results also showed a significant male predominance of stroke prevalence in CADASIL patients in accordance with epidemiological data showing a 45-55% age-adjusted male excess of ischemic stroke in the general population. [163, 193] This difference has been related to protective effects of oestrogens in women that can increase cerebral blood flow and vasoreactivity and show anti-inflammatory, antioxidant and anti-apoptotic properties in both animal models and human studies.[168, 169, 194, 195] The observation of a significant difference only before the usual age of menopause in the CADASIL population is in agreement with this hormonal hypothesis. Interestingly, in the present cohort, age at first stroke did not differ between men and women as previously reported in a smaller study.[170] This is in contrast with the 4 years younger age at first ischemic stroke reported in men in the general population.[163, 196] The limited size of the sample may prevent the detection of such a small difference in CADASIL patients. However, together with the lack of difference in the number of stroke events, these data may also indicate that female individuals are at lower risk of stroke but that the history of ischemic events does not actually differ between men and women once the first

stroke event has occurred. The lack of difference in the prevalence of TIAs between men and women contrasts with the gender effect observed for completed stroke. The information collected during the study about TIAs are, however, more prone to biases. Particularly, isolated auras frequently reported in CADASIL patients can be misdiagnosed as TIAs and vice versa. Elsewhere, recall biases are presumably more frequent for transient clinical manifestations than for stroke events, particularly in the presence of cognitive impairment.

Finally, we observed that men had lower scores in tests of executive functions and presented with more severe disability during the course of the disease. These results are only significant after 51 years of age, i.e. after several decades of accumulation of subcortical ischemic lesions. These results are in line with the large male predominance in apathy –a common symptom in CADASIL- already reported in a subgroup of the present cohort.[197] Although some psychological differences between men and women may partly explain this difference, recent data suggest that apathy mainly results from the accumulation of subcortical ischemic lesions leading to regional frontal cortical atrophy in CADASIL.[198] Accumulating evidence suggests that cerebral atrophy, the key marker of clinical severity in CADASIL, is related to the amount of subcortical ischemic lesion.[20] In the present study, the difference in clinical severity according to gender may be related to the more severe cerebral atrophy with a trend for a larger volume of lacunar infarcts in men compared to women. Interestingly, in this large cohort, the difference in cerebral atrophy was detected even before the 5th decade. The difference in vascular risk factors between sexes with only a small excess in alcohol intake in men is unlikely to be responsible for this difference. The neuroprotective role of female hormones may be involved in this gender-related difference.

There are a number of limitations in the present study. The age limit of 51 years chosen for stratified analysis was chosen based on the median value of age in the studied population that corresponds to the usual age at menopause in the general population. However, there are no data suggesting that the reproductive life differs in CADASIL patients from that observed in the general population. We also cannot exclude some biases in the collection of clinical data such as recall biases in the older subjects or in the presence of cognitive impairment or related to difficulties in discriminating migrainous auras from TIAs. The data were cross-sectional and the differences observed between men and women will need further confirmation in prospective longitudinal studies. Finally, the hypothesis of a protective role of ovarian hormones was not based on hormonal evaluation in the present

study. In particular, our data in no way indicate that hormone replacement therapy would be useful for stroke prevention in CADASIL since such a treatment was found to be detrimental in two large randomized controlled trials.[199, 200] The strengths of the study include the homogeneity of the population, the identical clinical and MRI protocol used in the two centers and the large population evaluated by trained physicians with expertise in both stroke and migraine.

5.2. ADC histogram in CADASIL

The main findings of our second study so far are that 1- MD and ADC histogram parameters are highly correlated, 2- CSF suppression has practically no effect on this correlation, 3- image artefact removal has negligible effect on ADC parameters and 4- the magnitude of the random scanner effect is superior to that of clinical scores on ADC parameters.

5.2.1. Comparison of ADC histogram to reference method

DTI-derived whole brain MD histograms emerged as reliable and precise markers of disease severity in cerebral small vessel disease also capable of monitoring its progression [103-108, 178, 181]. Although some studies used routine DWI-derived ADC histograms providing highly significant results [20], the different diffusion MR techniques have not been directly compared so far. Our study showed an excellent correlation between the corresponding MD and ADC histogram parameters (both with and without CSF suppression) in CADASIL indicating that the much simpler routine DWI may replace DTI in monitoring cSVD. The correlation was the most consistent for mean value so we would prefer this parameter to peak or height (either with or without CSF suppression).

5.2.2. Effects of post-hoc modifications (postprocessing)

Since the aim of the use of diffusion MR histograms is to quantify diffuse ultrastructural brain tissue damage, there has been a considerable effort to exclude effects that may "contaminate" or bias results such as the partial volume effect due to increased peripheral CSF spaces in atrophy, or imaging artefacts at the bone-air interface. For this purpose several methods of CSF suppression have been proposed: diffusion thresholding [20, 104, 177], fuzzy clustering-voxel based morphometry with varying degrees of cluster membership [106, 184], and FLAIR DWI [184, 201]. We used a relatively low diffusivity threshold (18 x 10-4 mm2/s) after careful visual assessment of different threshold values (ranging from 16 to 28 x 10-4 mm2/s) to exclude voxels containing CSF before histogram generation. CSF suppression did not change significantly MD-ADC correlations and had no effect at all on peak ADC; however it introduced a greater inter-scanner variability for mean ADC. Removal of bone-air artefacts and problematic top-bottom slices had only a negligible effect on ADC parameters thus we consider them unnecessary.

5.2.3. Scanner effect

The effect of using different scanners and imaging sequences and imaging-reimaging on diffusion data has been evaluated previously on a small number of healthy volunteers [183, 184]. These studies showed that the inter-scanner variability is greater than the inter-sequence variability, but both are relatively low, because diffusivity is a physical and not an MR property and thus less affected by technical differences [183]. Growing maximum b-values shifted the histograms to lower values, but scan-rescan results were not significantly different [184]. However these studies could not assess the variability introduced by technical differences in proportion to the variability related to disease. In our study we found that the magnitude of the scanner effect on ADC histogram parameters was significantly superior to that of clinical scores. Therefore data from different scanners in multicentre studies or from updated machines during the follow-up of a given patient are not directly comparable. If in practice it is not possible to use the same scanners, a quantification of scanner effect by the use of phantoms or a group of patients is necessary for data normalisation.

5.2.4. Utility of different ADC histogram parameters

Mean value, peak location and peak height of ADC histograms were evaluated. Kurtosis and skewness were highly correlated to peak height (analysis not shown) –all three parameters representing the form of the histogram curve-, and therefore left out from further evaluation.

Mean value seems to be the most useful parameter from many points of view: It is a continuous and thus more precise parameter containing more data than the peak which is a discrete parameter due to the use of bins. It shows a tighter correlation with the corresponding MD parameter than peak, and this correlation is linear (same in the whole range of data) unlike for height (descending B-A plot). It has been reported to be more sensitive to change than clinical scores during disease progression and to correlate with clinical scores both cross-sectionally and longitudinally more than the two other parameters [104-107]. Moreover it is less influenced by the random scanner effect as demonstrated in our study.

Atrophy has been shown to be a sensitive marker of global disease burden in CADASIL [129]. Both atrophy –through partial volume effect from increased CSF- and tissue disintegration increase mean diffusivity, while peak diffusivity being independent of CSF segmentation is less sensitive to atrophy related changes. This might partly be the reason why peak showed weaker correlation with clinical scores than mean value. Since partial volume

effect can be reduced otherwise (e.g. FLAIR DWI) we still prefer the use of mean value for its numerous advantages.

6. Conclusions

Results from our first study strongly support that gender largely influences the clinical and MRI phenotype of CADASIL. As observed in the general population, we found that women present more MA than men and less severe disability during the course of the disease. This difference that may be related to the protective role of ovarian hormones would need confirmation in prospective studies and specific biological assessments.

Whole brain ADC histogram parameters obtained from routine DWI without much postprocessing (CSF suppression, artefact removal) appear promising for monitoring diffuse small vessel disease such as CADASIL. However, given the significant random scanner effect on histogram parameters, the use of different scanners including technical updates may have major impact on the results and should be evaluated in a multicentre longitudinal trial.

7. Summary

Cerebral small vessel disease is characterized by lacunar stroke syndromes, deep intracerebral hemorrhage and progressive vascular dementia due to the pathology of small penetrating arteries of the brain. Its sporadic form related to hypertension has a growing importance in the aging society. Hereditary, monogenic variants affecting young individuals – such as CADASIL- are increasingly identified and serve as a pure genetic model of cSVD. New MRI techniques have greatly helped to explore cSVD. Diffusion MRI is useful in visualizing hyperacute LIs thus guiding acute phase therapy and etiologic diagnosis (DWI); and in detecting and quantifying the ultrastructural tissue damage (whole brain DTI histograms). Brain atrophy -a marker of cSVD- can be assessed with volumetric measures. These quantitative MRI techniques are more sensitive to the full spectrum of cSVD expressions and in detecting disease progression than other imaging parameters and clinical scores thus may provide surrogate markers for future therapeutic trials.

Migraine, stroke and vascular dementia differ in many aspects between men and women in the general population. Our first study aimed to evaluate the effect of gender on the main clinical and neuroimaging characteristics of CADASIL as a model disease. We found that migraine with aura was more frequent in women and stroke more frequent in men before the usual age of menopause. This difference seemed to vanish afterwards but resulted in more severe cognitive impairment and cerebral atrophy in men at the late stage of the disease. The presumable role of ovarian hormones in these gender-related differences remains to be explored.

DTI derived MD histogram metrics are already established markers of disease severity in cSVD in research settings. The aim of our second study was to evaluate whether ADC histograms from DWI used in routine clinical practice without significant postprocessing (CSF suppression, artefact removal), from different scanners can be used similarly to MD histograms in CADASIL. We found an excellent correlation between ADC and MD parameters. Correction of image artefacts did not alter ADC parameters significantly. In contrast, the magnitude of the scanner effect on ADC parameters was high and larger than that of clinical scores, sex and age. Therefore non-corrected ADC histogram parameters appear promising for assessing tissue damage in cSVD. However, given the important scanner effect, results from different scanners should be normalised to be comparable across centres and in individual patients.

8. Összefoglalás

Az agyi kisérbetegséget (aKB) a subcorticalis struktúrákat ellátó kis perforáló artériák megbetegedése okozta lacunaris stroke-ok, mély agyállományi vérzések ill. progreszív vascularis dementia jellemzi. A főleg hypertóniához társuló sporadikus formája növekvő epidemiológiai jelentőséggel bír az öregedő társadalmakban. Öröklődő, monogénes, fiatal betegeket érintő formái közül a CADASIL a legismertebb, amelyet az aKB tiszta, genetikai modelljének tekintünk. Az új MR technikák sokat segítettek az aKB megismerésében. A diffúziós MR különösen is hasznos a lacunaris infarctusok kimutatásában a hyperacut szakban, ezáltal segítve a korai etiológiai diagnózist (DWI); ill. a diffúz szövetkárosodás detektálásában és kvantifikálásában (egész agy DTI hisztogramok). A volumetriás módszerekkel megítélhető agyi atrófia az aKB egyik fontos markereként ismert. Ezen kvantitatív MR technikák alkalmasak az aKB okozta strukturális elváltozások teljes spektrumának megítélésére, valamint más képalkotó paramétereknél és klinikai mérőskáláknál érzékenyebbek a betegség progressziójára. Ennélfogva jövőbeli klinikai vizsgálatokban szerepelhetnek surrogate markerként.

A migrén, a stroke, ill. a vascularis dementia számos vonatkozásban eltér férfiak és nők között az általános népességben. Első vizsgálatunkban a CADASIL-ban mint modellbetegségben vizsgáltuk a nem hatását a betegség klinikai és MRI jellemzőire. Azt találtuk, hogy az aurás migrén gyakoribb volt nőkben a stroke pedig férfiakban a menopausa kora előtt. A különbség efölött a kor fölött eltűnni látszott, de a betegség későbbi stádiumában a férfiakban kifejezettebb kognitív deficitet és agyi atrófiát eredményezett. Feltettük, hogy ezen nemhez köthető különbségek kialakulásában az ovariális hormonoknak lehet szerepe.

A DTI alapú MD hisztogram paraméterek az aKB-nek már elfogadott markerei kísérleti körülmények között. Második vizsgálatunk célja az volt, hogy kiderítsük: vajon az egyszerűbb, rutin klinikai gyakorlatban használt DWI alapú ADC hisztogramok jelentősebb képkorrekció nélkül (liquorszuppresszió, műtermék eltávolítás), figyelembe véve az MR gépek rendszeres technikai frissítéseit az MD hisztogramokhoz hasonlóan használhatók-e CADASIL-ban. Kimagasló korrelációt találtunk az MD és ADC hisztogram paraméterek között függetlenül a liquormaszkolástól. A képi műtermékek korrigálása az ADC hisztogram paramétereket érdemben nem változtatta meg. Ugyanakkor az MR gépek különbözősége igen nagy hatással volt a paraméterekre, amely meghaladta a klinikai állapot, a nem és a kor

hatását is. A korrigálatlan ADC hisztogram tehát alkalmasnak tűnik az aKB okozta szövetkárosodás megítélésére, azonban a különböző gépeken készült eredmények normalizálásra van szükség az összehasonlíthatóság céljából.

References

1. Lammie GA. Pathology of small vessel stroke. *Brit. Med. Bul*. 2000;56:296-306
2. Hachinski V. World stroke day 2008: "Little strokes, big trouble". *Stroke,* 2008;39:2407-2420
3. Thompson CS, Hakim AM. Living beyond our physiological means: Small vessel disease of the brain is an expression of a systemic failure in arteriolar function: A unifying hypothesis. *Stroke,* 2009;40:e322-330
4. Vermeer SE, Longstreth WT, Jr., Koudstaal PJ. Silent brain infarcts: A systematic review. *Lancet Neurol*. 2007;6:611-619
5. Bryan RN, Wells SW, Miller TJ, Elster AD, Jungreis CA, Poirier VC, Lind BK, Manolio TA. Infarctlike lesions in the brain: Prevalence and anatomic characteristics at mr imaging of the elderly--data from the cardiovascular health study. *Radiology,* 1997;202:47-54
6. Bamford J, Sandercock P, Jones L, Warlow C. The natural history of lacunar infarction: The oxfordshire community stroke project. *Stroke,* 1987;18:545-551
7. Petty GW, Brown RD, Jr., Whisnant JP, Sicks JD, O'Fallon WM, Wiebers DO. Ischemic stroke subtypes: A population-based study of incidence and risk factors. *Stroke,* 1999;30:2513-2516
8. Sacco S, Marini C, Totaro R, Russo T, Cerone D, Carolei A. A population-based study of the incidence and prognosis of lacunar stroke. *Neurology,* 2006;66:1335-1338
9. Joutel A, Corpechot C, Ducros A, Vahedi K, Chabriat H, Mouton P, Alamowitch S, Domenga V, Cecillion M, Marechal E, Maciazek J, Vayssiere C, Cruaud C, Cabanis EA, Ruchoux MM, Weissenbach J, Bach JF, Bousser MG, Tournier-Lasserve E. Notch3 mutations in CADASIL, a hereditary adult-onset condition causing stroke and dementia. *Nature,* 1996;383:707-710
10. Artavanis-Tsakonas S, Rand MD, Lake RJ. Notch signaling: Cell fate control and signal integration in development. *Science,* 1999;284:770-776
11. Pantoni L. Cerebral small vessel disease: From pathogenesis and clinical characteristics to therapeutic challenges. *Lancet Neurol*.9:689-701
12. Herman LH, Ostrowski AZ, Gurdjian ES. Perforating branches of the middle cerebral artery. An anatomical study. *Arch Neurol*. 1963;8:32-34

13. Kaplan HA. The lateral perforating branches of the anterior and middle cerebral arteries. *J. Neurosurg*. 1965;23:305-310
14. Marinkovic SV, Milisavljevic MM, Kovacevic MS, Stevic ZD. Perforating branches of the middle cerebral artery. Microanatomy and clinical significance of their intracerebral segments. *Stroke,* 1985;16:1022-1029
15. Umansky F, Gomes FB, Dujovny M, Diaz FG, Ausman JI, Mirchandani HG, Berman SK. The perforating branches of the middle cerebral artery. A microanatomical study. *J. Neurosurg.* 1985;62:261-268
16. Pantoni L. Pathophysiology of age-related cerebral white matter changes. *Cerebrovasc. Dis.* 2002;13 Suppl 2:7-10
17. Fisher CM. Lacunar strokes and infarcts: A review. *Neurology,* 1982;32:871-876
18. Fazekas F, Kleinert R, Roob G, Kleinert G, Kapeller P, Schmidt R, Hartung HP. Histopathologic analysis of foci of signal loss on gradient-echo T2*-weighted MR images in patients with spontaneous intracerebral hemorrhage: Evidence of microangiopathy-related microbleeds. *Am. J. Neuroradiol*. 1999;20:637-642
19. Greenberg SM, Nandigam RN, Delgado P, Betensky RA, Rosand J, Viswanathan A, Frosch MP, Smith EE. Microbleeds versus macrobleeds: Evidence for distinct entities. *Stroke,* 2009;40:2382-2386
20. Jouvent E, Viswanathan A, Mangin JF, O'Sullivan M, Guichard JP, Gschwendtner A, Cumurciuc R, Buffon F, Peters N, Pachai C, Bousser MG, Dichgans M, Chabriat H. Brain atrophy is related to lacunar lesions and tissue microstructural changes in CADASIL. *Stroke,* 2007;38:1786-1790
21. Gunda B VG, Bereczki D. Multimodal MRI of cerebral small vessel disease. *Neuroimaging –Clinical Applications*. 2012:277-300
22. Gunda B RG, Várallyay Gy, Bereczki D. Challenges in diagnosing cerebral lacunar infarcts. *Curr. Med. Imaging Rev*. 2009;5:75-84
23. Brant-Zawadzki M, Atkinson D, Detrick M, Bradley WG, Scidmore G. Fluid-attenuated inversion recovery (FLAIR) for assessment of cerebral infarction. Initial clinical experience in 50 patients. *Stroke,* 1996;27:1187-1191
24. Ricci PE, Burdette JH, Elster AD, Reboussin DM. A comparison of fast spin-echo, fluid-attenuated inversion-recovery, and diffusion-weighted mr imaging in the first 10 days after cerebral infarction. *Am. J. Neuroradiol.* 1999;20:1535-1542

25. Lansberg MG, Thijs VN, O'Brien MW, Ali JO, de Crespigny AJ, Tong DC, Moseley ME, Albers GW. Evolution of apparent diffusion coefficient, diffusion-weighted, and t2-weighted signal intensity of acute stroke. *Am. J. Neuroradiol*. 2001;22:637-644

26. Mintorovitch J, Moseley ME, Chileuitt L, Shimizu H, Cohen Y, Weinstein PR. Comparison of diffusion- and t2-weighted MRI for the early detection of cerebral ischemia and reperfusion in rats. *Magn Reson. Med*. 1991;18:39-50

27. Hjort N, Christensen S, Solling C, Ashkanian M, Wu O, Rohl L, Gyldensted C, Andersen G, Ostergaard L. Ischemic injury detected by diffusion imaging 11 minutes after Stroke, *Ann. Neurol*. 2005;58:462-465

28. Guadagno JV, Jones PS, Fryer TD, Barret O, Aigbirhio FI, Carpenter TA, Price CJ, Gillard JH, Warburton EA, Baron JC. Local relationships between restricted water diffusion and oxygen consumption in the ischemic human brain. *Stroke,* 2006;37:1741-1748

29. Hoehn-Berlage M, Norris DG, Kohno K, Mies G, Leibfritz D, Hossmann KA. Evolution of regional changes in apparent diffusion coefficient during focal ischemia of rat brain: The relationship of quantitative diffusion nmr imaging to reduction in cerebral blood flow and metabolic disturbances. *J. Cereb. Blood Flow Metab*. 1995;15:1002-1011

30. Lin W, Lee JM, Lee YZ, Vo KD, Pilgram T, Hsu CY. Temporal relationship between apparent diffusion coefficient and absolute measurements of cerebral blood flow in acute stroke patients. *Stroke,* 2003;34:64-70

31. Schlaug G, Siewert B, Benfield A, Edelman RR, Warach S. Time course of the apparent diffusion coefficient (adc) abnormality in human stroke. *Neurology,* 1997;49:113-119

32. Munoz Maniega S, Bastin ME, Armitage PA. A quantitative comparison of two methods to correct eddy current-induced distortions in DT-MRI. *Magnetic resonance imaging*, 2007;25:341-349

33. Knight RA, Dereski MO, Helpern JA, Ordidge RJ, Chopp M. Magnetic resonance imaging assessment of evolving focal cerebral ischemia. Comparison with histopathology in rats. *Stroke,* 1994;25:1252-1261; discussion 1261-1252

34. Burdette JH, Elster AD, Ricci PE. Acute cerebral infarction: Quantification of spin-density and T2 shine-through phenomena on diffusion-weighted MR images. *Radiology*, 1999;212:333-339

35. Geijer B, Sundgren PC, Lindgren A, Brockstedt S, Stahlberg F, Holtas S. The value of b required to avoid T2 shine-through from old lucunar infarcts in diffusion-weighted imaging. *Neuroradiology*, 2001;43:511-517
36. Lovblad KO, Laubach HJ, Baird AE, Curtin F, Schlaug G, Edelman RR, Warach S. Clinical experience with diffusion-weighted MR in patients with acute stroke. *Am. J. Neuroradiol.* 1998;19:1061-1066
37. Lie C, Hirsch JG, Rossmanith C, Hennerici MG, Gass A. Clinicotopographical correlation of corticospinal tract stroke: A color-coded diffusion tensor imaging study. *Stroke*, 2004;35:86-92
38. Pajevic S, Pierpaoli C. Color schemes to represent the orientation of anisotropic tissues from diffusion tensor data: Application to white matter fiber tract mapping in the human brain. *Magn Reson Med*. 1999;42:526-540
39. Wakana S, Jiang H, Nagae-Poetscher LM, van Zijl PC, Mori S. Fiber tract-based atlas of human white matter anatomy. *Radiology*, 2004;230:77-87
40. Lai C, Zhang SZ, Liu HM, Zhou YB, Zhang YY, Zhang QW, Han GC. White matter tractography by diffusion tensor imaging plays an important role in prognosis estimation of acute lacunar infarctions. *Br J Radiol*. 2007;80:782-789
41. Lee JS, Han MK, Kim SH, Kwon OK, Kim JH. Fiber tracking by diffusion tensor imaging in corticospinal tract stroke: Topographical correlation with clinical symptoms. *Neuroimage*, 2005;26:771-776
42. Yamada K, Mori S, Nakamura H, Ito H, Kizu O, Shiga K, Yoshikawa K, Makino M, Yuen S, Kubota T, Tanaka O, Nishimura T. Fiber-tracking method reveals sensorimotor pathway involvement in stroke patients. *Stroke*, 2003;34:E159-162
43. Norrving B. Lacunar infarcts: No black holes in the brain are benign. *Practical Neurology*, 2008;8:222-228
44. Cho AH, Kang DW, Kwon SU, Kim JS. Is 15 mm size criterion for lacunar infarction still valid? A study on strictly subcortical middle cerebral artery territory infarction using diffusion-weighted MRI. *Cerebrovasc Dis*. 2007;23:14-19
45. Kang DW, Chalela JA, Ezzeddine MA, Warach S. Association of ischemic lesion patterns on early diffusion-weighted imaging with toast stroke subtypes. *Arch. Neurol*. 2003;60:1730-1734
46. Wessels T, Rottger C, Jauss M, Kaps M, Traupe H, Stolz E. Identification of embolic stroke patterns by diffusion-weighted MRI in clinically defined lacunar stroke syndromes. *Stroke*, 2005;36:757-761

47. Donnan GA, Bladin PF, Berkovic SF, Longley WA, Saling MM. The stroke syndrome of striatocapsular infarction. *Brain*, 1991;114 (Pt 1A):51-70
48. Gerraty RP, Parsons MW, Barber PA, Darby DG, Desmond PM, Tress BM, Davis SM. Examining the lacunar hypothesis with diffusion and perfusion magnetic resonance imaging. *Stroke,* 2002;33:2019-2024
49. Wessels T, Wessels C, Ellsiepen A, Reuter I, Trittmacher S, Stolz E, Jauss M. Contribution of diffusion-weighted imaging in determination of stroke etiology. *Am. J. Neuroradiol.* 2006;27:35-39
50. Chowdhury D, Wardlaw JM, Dennis MS. Are multiple acute small subcortical infarctions caused by embolic mechanisms? *J. Neurol. Neurosurg. Psychiatry*. 2004;75:1416-1420
51. Momjian-Mayor I, Baron JC. The pathophysiology of watershed infarction in internal carotid artery disease: Review of cerebral perfusion studies. *Stroke,* 2005;36:567-577
52. Krapf H, Widder B, Skalej M. Small rosarylike infarctions in the centrum ovale suggest hemodynamic failure. *Am. J. Neuroradiol.* 1998;19:1479-1484
53. Scarpelli M, Salvolini U, Diamanti L, Montironi R, Chiaromoni L, Maricotti M. MRI and pathological examination of post-mortem brains: The problem of white matter high signal areas. *Neuroradiology,* 1994;36:393-398
54. Gilbert JJ, Sadler M. Unsuspected multiple sclerosis. *Arch. Neurol*. 1983;40:533-536
55. Kirkpatrick JB, Hayman LA. White-matter lesions in mr imaging of clinically healthy brains of elderly subjects: Possible pathologic basis. *Radiology*, 1987;162:509-511
56. Munoz DG, Hastak SM, Harper B, Lee D, Hachinski VC. Pathologic correlates of increased signals of the centrum ovale on magnetic resonance imaging. *Arch. Neurol*. 1993;50:492-497
57. Haddad FS, Abla A, Allam C. Ependymal brain cyst. *Surg. Neurol.*, 1982;18:246-249
58. Braffman BH, Zimmerman RA, Trojanowski JQ, Gonatas NK, Hickey WF, Schlaepfer WW. Brain mr: Pathologic correlation with gross and histopathology. 2. Hyperintense white-matter foci in the elderly. *Am. J. Roentgenol*. 1988;151:559-566
59. Weller RO, Kida S, Zhang ET. Pathways of fluid drainage from the brain--morphological aspects and immunological significance in rat and man. *Brain pathology,* 1992;2:277-284
60. Jungreis CA, Kanal E, Hirsch WL, Martinez AJ, Moossy J. Normal perivascular spaces mimicking lacunar infarction: Mr imaging. *Radiology,* 1988;169:101-104

61. Bokura H, Kobayashi S, Yamaguchi S. Distinguishing silent lacunar infarction from enlarged Virchow-Robin spaces: A magnetic resonance imaging and pathological study. *J. Neurol*. 1998;245:116-122
62. Groeschel S, Chong WK, Surtees R, Hanefeld F. Virchow-Robin spaces on magnetic resonance images: Normative data, their dilatation, and a review of the literature. *Neuroradiology*, 2006;48:745-754
63. Rouhl RP, van Oostenbrugge RJ, Knottnerus IL, Staals JE, Lodder J. Virchow-Robin spaces relate to cerebral small vessel disease severity. *J. Neurol*. 2008
64. Heier LA, Bauer CJ, Schwartz L, Zimmerman RD, Morgello S, Deck MD. Large Virchow-Robin spaces: MR-clinical correlation. *Am. J. Neuroradiol.* 1989;10:929-936
65. Hiroki M, Miyashita K. Linear hyperintensity objects on magnetic resonance imaging related to hypertension. *Cerebrovasc. Dis*. 2001;11:164-168
66. Maclullich AM, Wardlaw JM, Ferguson KJ, Starr JM, Seckl JR, Deary IJ. Enlarged perivascular spaces are associated with cognitive function in healthy elderly men. *J. Neurol. Neurosurg. Psychiatry*. 2004;75:1519-1523
67. Patankar TF, Mitra D, Varma A, Snowden J, Neary D, Jackson A. Dilatation of the Virchow-Robin space is a sensitive indicator of cerebral microvascular disease: Study in elderly patients with dementia. *Am. J. Neuroradiol.* 2005;26:1512-1520
68. Cumurciuc R, Guichard JP, Reizine D, Gray F, Bousser MG, Chabriat H. Dilation of Virchow-Robin spaces in CADASIL. *Eur. J. Neurol*. 2006;13:187-190
69. Erkinjuntti T, Benavente O, Eliasziw M, Munoz DG, Sulkava R, Haltia M, Hachinski V. Diffuse vacuolization (spongiosis) and arteriolosclerosis in the frontal white matter occurs in vascular dementia. *Arch. Neurol*. 1996;53:325-332
70. Barkhof F. Enlarged Virchow-Robin spaces: Do they matter? *J. Neurol. Neurosurg. Psychiatry*, 2004;75:1516-1517
71. Bots ML, Looman SJ, Koudstaal PJ, Hofman A, Hoes AW, Grobbee DE. Prevalence of stroke in the general population. The Rotterdam study. *Stroke*, 1996;27:1499-1501
72. Mittelmark MB, Psaty BM, Rautaharju PM, Fried LP, Borhani NO, Tracy RP, Gardin JM, O'Leary DH. Prevalence of cardiovascular diseases among older adults. The cardiovascular health study. *Am. J. Epidemiol*. 1993;137:311-317
73. Vermeer SE, Den Heijer T, Koudstaal PJ, Oudkerk M, Hofman A, Breteler MM. Incidence and risk factors of silent brain infarcts in the population-based Rotterdam scan study. *Stroke*, 2003;34:392-396

74. Vermeer SE, Koudstaal PJ, Oudkerk M, Hofman A, Breteler MM. Prevalence and risk factors of silent brain infarcts in the population-based Rotterdam scan study. *Stroke,* 2002;33:21-25

75. Norrving B. Long-term prognosis after lacunar infarction. *Lancet Neurol*. 2003;2:238-245

76. Longstreth WT, Jr., Arnold AM, Beauchamp NJ, Jr., Manolio TA, Lefkowitz D, Jungreis C, Hirsch CH, O'Leary DH, Furberg CD. Incidence, manifestations, and predictors of worsening white matter on serial cranial magnetic resonance imaging in the elderly: The cardiovascular health study. *Stroke,* 2005;36:56-61

77. Hachinski VC, Potter P, Merskey H. Leuko-araiosis. *Arch. Neurol.* 1987;44:21-23

78. Marshall VG, Bradley WG, Jr., Marshall CE, Bhoopat T, Rhodes RH. Deep white matter infarction: Correlation of mr imaging and histopathologic findings. *Radiology,* 1988;167:517-522

79. Revesz T, Hawkins CP, du Boulay EP, Barnard RO, McDonald WI. Pathological findings correlated with magnetic resonance imaging in subcortical arteriosclerotic encephalopathy (binswanger's disease). *J. Neurol. Neurosurg. Psychiatry,* 1989;52:1337-1344

80. Fazekas F, Kleinert R, Offenbacher H, Schmidt R, Kleinert G, Payer F, Radner H, Lechner H. Pathologic correlates of incidental MRI white matter signal hyperintensities. *Neurology,* 1993;43:1683-1689

81. Fernando MS, O'Brien JT, Perry RH, English P, Forster G, McMeekin W, Slade JY, Golkhar A, Matthews FE, Barber R, Kalaria RN, Ince PG. Comparison of the pathology of cerebral white matter with post-mortem magnetic resonance imaging (MRI) in the elderly brain. *Neuropath. Appl. Neuro*. 2004;30:385-395

82. Bartynski WS. Posterior reversible encephalopathy syndrome, part 1: Fundamental imaging and clinical features. *Am. J. Neuroradiol.* 2008;29:1036-1042

83. Costello DJ, Eichler AF, Eichler FS. Leukodystrophies: Classification, diagnosis, and treatment. *The neurologist*. 2009;15:319-328

84. Matthews PM, Tampieri D, Berkovic SF, Andermann F, Silver K, Chityat D, Arnold DL. Magnetic resonance imaging shows specific abnormalities in the MELAS syndrome. *Neurology,* 1991;41:1043-1046

85. Fazekas F CJ, Alavi A, Hurtig HI, Zimmerman RA. MR signal abnormalities at 1.5T in Alzheimer's dementia and normal aging. *Am J Roentgenol*. 1987

86. Schmidt R, Fazekas F, Kapeller P, Schmidt H, Hartung HP. MRI white matter hyperintensities: Three-year follow-up of the austrian stroke prevention study. *Neurology*, 1999;53:132-139

87. Scheltens P, Barkhof F, Leys D, Pruvo JP, Nauta JJ, Vermersch P, Steinling M, Valk J. A semiquantative rating scale for the assessment of signal hyperintensities on magnetic resonance imaging. *J. Neurol. Sci*. 1993;114:7-12

88. Wahlund LO, Barkhof F, Fazekas F, Bronge L, Augustin M, Sjogren M, Wallin A, Ader H, Leys D, Pantoni L, Pasquier F, Erkinjuntti T, Scheltens P. A new rating scale for age-related white matter changes applicable to MRI and ct. *Stroke,* 2001;32:1318-1322

89. Kapeller P, Schmidt R, Enzinger C, Ropele S, Fazekas F. CT and MRI rating of white matter changes. *J. Neural. Transm*. 2002:41-45

90. Anbeek P, Vincken KL, van Osch MJ, Bisschops RH, van der Grond J. Probabilistic segmentation of white matter lesions in MR imaging. *NeuroImage*. 2004;21:1037-1044

91. Sachdev P, Cathcart S, Shnier R, Wen W, Brodaty H. Reliability and validity of ratings of signal hyperintensities on MRI by visual inspection and computerised measurement. *Psychiatry research.* 1999;92:103-115

92. Gouw AA, van der Flier WM, van Straaten EC, Pantoni L, Bastos-Leite AJ, Inzitari D, Erkinjuntti T, Wahlund LO, Ryberg C, Schmidt R, Fazekas F, Scheltens P, Barkhof. Reliability and sensitivity of visual scales versus volumetry for evaluating white matter hyperintensity progression. *Cerebrovasc. Dis.* 2008;25:247-253

93. de Groot JC, de Leeuw FE, Oudkerk M, van Gijn J, Hofman A, Jolles J, Breteler MM. Cerebral white matter lesions and cognitive function: The Rotterdam scan study. *Ann. Neurol.* 2000;47:145-151

94. van Straaten EC, Fazekas F, Rostrup E, Scheltens P, Schmidt R, Pantoni L, Inzitari D, Waldemar G, Erkinjuntti T, Mantyla R, Wahlund LO, Barkhof F. Impact of white matter hyperintensities scoring method on correlations with clinical data: The LADIS study. *Stroke,* 2006;37:836-840

95. Nebes RD, Meltzer CC, Whyte EM, Scanlon JM, Halligan EM, Saxton JA, Houck PR, Boada FE, Dekosky ST. The relation of white matter hyperintensities to cognitive performance in the normal old: Education matters. *Neuropsy. Develop. Cogn*. 2006;13:326-340

96. Rovaris M, Iannucci G, Cercignani M, Sormani MP, De Stefano N, Gerevini S, Comi G, Filippi M. Age-related changes in conventional, magnetization transfer, and diffusion-tensor MR imaging findings: Study with whole-brain tissue histogram analysis. *Radiology*, 2003;227:731-738

97. Benedetti B, Charil A, Rovaris M, Judica E, Valsasina P, Sormani MP, Filippi M. Influence of aging on brain gray and white matter changes assessed by conventional, MT, and DT MRI. *Neurology*, 2006;66:535-539

98. Horsfield MA, Jones DK. Applications of diffusion-weighted and diffusion tensor MRI to white matter diseases - a review. *NMR in biomedicine*. 2002;15:570-577

99. Mascalchi M, Filippi M, Floris R, Fonda C, Gasparotti R, Villari N. Diffusion-weighted MR of the brain: Methodology and clinical application. *La Radiologia medica*. 2005;109:155-197

100. Beaulieu C. The basis of anisotropic water diffusion in the nervous system - a technical review. *NMR in biomedicine*. 2002;15:435-455

101. O'Sullivan M, Summers PE, Jones DK, Jarosz JM, Williams SC, Markus HS. Normal-appearing white matter in ischemic leukoaraiosis: A diffusion tensor MRI study. *Neurology*, 2001;57:2307-2310

102. Molko N, Pappata S, Mangin JF, Poupon C, Vahedi K, Jobert A, LeBihan D, Bousser MG, Chabriat H. Diffusion tensor imaging study of subcortical gray matter in CADASIL. *Stroke*, 2001;32:2049-2054

103. Chabriat H, Pappata S, Poupon C, Clark CA, Vahedi K, Poupon F, Mangin JF, Pachot-Clouard M, Jobert A, Le Bihan D, Bousser MG. Clinical severity in CADASIL related to ultrastructural damage in white matter: In vivo study with diffusion tensor MRI. *Stroke*, 1999;30:2637-2643

104. Holtmannspotter M, Peters N, Opherk C, Martin D, Herzog J, Bruckmann H, Samann P, Gschwendtner A, Dichgans M. Diffusion magnetic resonance histograms as a surrogate marker and predictor of disease progression in CADASIL: A two-year follow-up study. *Stroke*, 2005;36:2559-2565

105. Molko N, Pappata S, Mangin JF, Poupon F, LeBihan D, Bousser MG, Chabriat H. Monitoring disease progression in CADASIL with diffusion magnetic resonance imaging: A study with whole brain histogram analysis. *Stroke*, 2002;33:2902-2908

106. Nitkunan A, Barrick TR, Charlton RA, Clark CA, Markus HS. Multimodal MRI in cerebral small vessel disease: Its relationship with cognition and sensitivity to change over time. *Stroke*, 2008;39:1999-2005

107. Charlton RA, Schiavone F, Barrick TR, Morris RG, Markus HS. Diffusion tensor imaging detects age related white matter change over a 2 year follow-up which is associated with working memory decline. *J. Neurol. Neurosurg. Psychiatry,* 81:13-19

108. Della Nave R, Foresti S, Pratesi A, Ginestroni A, Inzitari M, Salvadori E, Giannelli M, Diciotti S, Inzitari D, Mascalchi M. Whole-brain histogram and voxel-based analyses of diffusion tensor imaging in patients with leukoaraiosis: Correlation with motor and cognitive impairment. *Am. J. Neuroradiol.* 2007;28:1313-1319

109. Offenbacher H, Fazekas F, Schmidt R, Koch M, Fazekas G, Kapeller P. MR of cerebral abnormalities concomitant with primary intracerebral hematomas. *Am. J. Neuroradiol.* 1996;17:573-578

110. Greenberg SM, Finklestein SP, Schaefer PW. Petechial hemorrhages accompanying lobar hemorrhage: Detection by gradient-echo MRI. *Neurology,* 1996;46:1751-1754

111. Ripoll MA, Siosteen B, Hartman M, Raininko R. MR detectability and appearance of small experimental intracranial hematomas at 1.5 T and 0.5 T. A 6-7-month follow-up study. *Acta Radiol*. 2003;44:199-205

112. Tanaka A, Ueno Y, Nakayama Y, Takano K, Takebayashi S. Small chronic hemorrhages and ischemic lesions in association with spontaneous intracerebral hematomas. *Stroke,* 1999;30:1637-1642

113. Viswanathan A, Chabriat H. Cerebral microhemorrhage. *Stroke,* 2006;37:550-555

114. Fiehler J. Cerebral microbleeds: Old leaks and new haemorrhages. *Int. J. Stroke,* 2006;1:122-130

115. Cordonnier C, Al-Shahi Salman R, Wardlaw J. Spontaneous brain microbleeds: Systematic review, subgroup analyses and standards for study design and reporting. *Brain*, 2007;130:1988-2003

116. Lee SH, Kwon SJ, Kim KS, Yoon BW, Roh JK. Cerebral microbleeds in patients with hypertensive Stroke, Topographical distribution in the supratentorial area. *J. Neurol,* 2004;251:1183-1189

117. Chalela JA, Kang DW, Warach S. Multiple cerebral microbleeds: MRI marker of a diffuse hemorrhage-prone state. *J. Neuroimaging*. 2004;14:54-57

118. Derex L, Nighoghossian N, Hermier M, Adeleine P, Philippeau F, Honnorat J, Yilmaz H, Dardel P, Froment JC, Trouillas P. Thrombolysis for ischemic stroke in patients with old microbleeds on pretreatment MRI. *Cerebrovasc. Dis.* 2004;17:238-241

119. Kakuda W, Thijs VN, Lansberg MG, Bammer R, Wechsler L, Kemp S, Moseley ME, Marks MP, Albers GW. Clinical importance of microbleeds in patients receiving iv thrombolysis. *Neurology,* 2005;65:1175-1178

120. Kidwell CS, Saver JL, Villablanca JP, Duckwiler G, Fredieu A, Gough K, Leary MC, Starkman S, Gobin YP, Jahan R, Vespa P, Liebeskind DS, Alger JR, Vinuela F. Magnetic resonance imaging detection of microbleeds before thrombolysis: An emerging application. *Stroke,* 2002;33:95-98

121. Nighoghossian N, Hermier M, Adeleine P, Blanc-Lasserre K, Derex L, Honnorat J, Philippeau F, Dugor JF, Froment JC, Trouillas P. Old microbleeds are a potential risk factor for cerebral bleeding after ischemic stroke: A gradient-echo T2*-weighted brain MRI study. *Stroke,* 2002;33:735-742

122. Enzinger C, Fazekas F, Matthews PM, Ropele S, Schmidt H, Smith S, Schmidt R. Risk factors for progression of brain atrophy in aging: Six-year follow-up of normal subjects. *Neurology,* 2005;64:1704-1711

123. Karas GB, Scheltens P, Rombouts SA, Visser PJ, van Schijndel RA, Fox NC, Barkhof F. Global and local gray matter loss in mild cognitive impairment and Alzheimer's disease. *NeuroImage*. 2004;23:708-716

124. Zivadinov R, Sepcic J, Nasuelli D, De Masi R, Bragadin LM, Tommasi MA, Zambito-Marsala S, Moretti R, Bratina A, Ukmar M, Pozzi-Mucelli RS, Grop A, Cazzato G, Zorzon M. A longitudinal study of brain atrophy and cognitive disturbances in the early phase of relapsing-remitting multiple sclerosis. *J. Neurol. Neurosurg. Psychiatry,* 2001;70:773-780

125. Kraemer M, Schormann T, Hagemann G, Qi B, Witte OW, Seitz RJ. Delayed shrinkage of the brain after ischemic stroke: Preliminary observations with voxel-guided morphometry. *J. Neuroimaging*. 2004;14:265-272

126. Schmidt R, Ropele S, Enzinger C, Petrovic K, Smith S, Schmidt H, Matthews PM, Fazekas F. White matter lesion progression, brain atrophy, and cognitive decline: The austrian stroke prevention study. *Ann. Neurol.* 2005;58:610-616

127. Preul C, Lohmann G, Hund-Georgiadis M, Guthke T, von Cramon DY. Morphometry demonstrates loss of cortical thickness in cerebral microangiopathy. *J. Neurol,* 2005;252:441-447

128. Seshadri S, Wolf PA, Beiser A, Elias MF, Au R, Kase CS, D'Agostino RB, DeCarli C. Stroke risk profile, brain volume, and cognitive function: The Framingham offspring study. *Neurology,* 2004;63:1591-1599

129. Viswanathan A, Godin O, Jouvent E, O'Sullivan M, Gschwendtner A, Peters N, Duering M, Guichard JP, Holtmannspotter M, Dufouil C, Pachai C, Bousser MG, Dichgans M, Chabriat H. Impact of MRI markers in subcortical vascular dementia: A multi-modal analysis in CADASIL. *Neurobiol. Aging*. 31:1629-1636

130. Fein G, Di Sclafani V, Tanabe J, Cardenas V, Weiner MW, Jagust WJ, Reed BR, Norman D, Schuff N, Kusdra L, Greenfield T, Chui H. Hippocampal and cortical atrophy predict dementia in subcortical ischemic vascular disease. *Neurology,* 2000;55:1626-1635

131. Jouvent E, Mangin JF, Porcher R, Viswanathan A, O'Sullivan M, Guichard JP, Dichgans M, Bousser MG, Chabriat H. Cortical changes in cerebral small vessel diseases: A 3d MRI study of cortical morphology in CADASIL. *Brain,* 2008;131:2201-2208

132. Viswanathan A, Gray F, Bousser MG, Baudrimont M, Chabriat H. Cortical neuronal apoptosis in CADASIL. *Stroke*, 2006;37:2690-2695

133. Rao DG, Lyons PR. Wallerian degeneration of the pyramidal tract after a thrombotic stroke. *J. Neurol. Neurosurg. Psychiatry*, 1998;65:944

134. Jouvent E, Viswanathan A, Chabriat H. Cerebral atrophy in cerebrovascular disorders. *J Neuroimaging*.20:213-218

135. Chabriat H, Joutel A, Dichgans M, Tournier-Lasserve E, Bousser MG. CADASIL. *Lancet Neurol*. 2009;8:643-653

136. Chabriat H, Levy C, Taillia H, Iba-Zizen MT, Vahedi K, Joutel A, Tournier-Lasserve E, Bousser MG. Patterns of MRI lesions in CADASIL. *Neurology*, 1998;51:452-457

137. Auer DP, Putz B, Gossl C, Elbel G, Gasser T, Dichgans M. Differential lesion patterns in CADASIL and sporadic subcortical arteriosclerotic encephalopathy: MR imaging study with statistical parametric group comparison. *Radiology*, 2001;218:443-451

138. Markus HS, Martin RJ, Simpson MA, Dong YB, Ali N, Crosby AH, Powell JF. Diagnostic strategies in CADASIL. *Neurology,* 2002;59:1134-1138

139. O'Sullivan M, Jarosz JM, Martin RJ, Deasy N, Powell JF, Markus HS. MRI hyperintensities of the temporal lobe and external capsule in patients with CADASIL. *Neurology,* 2001;56:628-634

140. Yamamoto Y, Craggs L, Baumann M, Kalimo H, Kalaria RN. Review: Molecular genetics and pathology of hereditary small vessel diseases of the brain. *Neuropath. Appl. Neuro*. 2011;37:94-113

141. Arima K, Yanagawa S, Ito N, Ikeda S. Cerebral arterial pathology of CADASIL and CARASIL (Maeda syndrome). *Neuropathology*, 2003;23:327-334

142. Yanagawa S, Ito N, Arima K, Ikeda S. Cerebral autosomal recessive arteriopathy with subcortical infarcts and leukoencephalopathy. *Neurology*, 2002;58:817-820

143. Hara K, Shiga A, Fukutake T, Nozaki H, Miyashita A, Yokoseki A, Kawata H, Koyama A, Arima K, Takahashi T, Ikeda M, Shiota H, Tamura M, Shimoe Y, Hirayama M, Arisato T, Yanagawa S, Tanaka A, Nakano I, Ikeda S, Yoshida Y, Yamamoto T, Ikeuchi T, Kuwano R, Nishizawa M, Tsuji S, Onodera O. Association of HTRA1 mutations and familial ischemic cerebral small-vessel disease. *The New England journal of medicine*. 2009;360:1729-1739

144. Jen J, Cohen AH, Yue Q, Stout JT, Vinters HV, Nelson S, Baloh RW. Hereditary endotheliopathy with retinopathy, nephropathy, and stroke (HERNS). *Neurology*, 1997;49:1322-1330

145. Grand MG, Kaine J, Fulling K, Atkinson J, Dowton SB, Farber M, Craver J, Rice K. Cerebroretinal vasculopathy. A new hereditary syndrome. *Ophthalmology*, 1988;95:649-659

146. Terwindt GM, Haan J, Ophoff RA, Groenen SM, Storimans CW, Lanser JB, Roos RA, Bleeker-Wagemakers EM, Frants RR, Ferrari MD. Clinical and genetic analysis of a large dutch family with autosomal dominant vascular retinopathy, migraine and raynaud's phenomenon. *Brain*, 1998;121 (Pt 2):303-316

147. Richards A, van den Maagdenberg AM, Jen JC, Kavanagh D, Bertram P, Spitzer D, Liszewski MK, Barilla-Labarca ML, Terwindt GM, Kasai Y, McLellan M, Grand MG, Vanmolkot KR, de Vries B, Wan J, Kane MJ, Mamsa H, Schafer R, Stam AH, Haan J, de Jong PT, Storimans CW, van Schooneveld MJ, Oosterhuis JA, Gschwendter A, Dichgans M, Kotschet KE, Hodgkinson S, Hardy TA, Delatycki MB, Hajj-Ali RA, Kothari PH, Nelson SF, Frants RR, Baloh RW, Ferrari MD, Atkinson JP. C-terminal truncations in human 3'-5' DNA exonuclease trex1 cause autosomal dominant retinal vasculopathy with cerebral leukodystrophy. *Nature genetics*, 2007;39:1068-1070

148. Gould DB, Phalan FC, van Mil SE, Sundberg JP, Vahedi K, Massin P, Bousser MG, Heutink P, Miner JH, Tournier-Lasserve E, John SW. Role of col4a1 in small-vessel disease and hemorrhagic Stroke, *The New England journal of medicine*. 2006;354:1489-1496

149. Vahedi K, Alamowitch S. Clinical spectrum of type iv collagen (col4a1) mutations: A novel genetic multisystem disease. *Curr. Opin. Neurol.*, 2011;24:63-68

150. Pavlovic AM, Zidverc-Trajkovic J, Milovic MM, Pavlovic DM, Jovanovic Z, Mijajlovic M, Petrovic M, Kostic VS, Sternic N. Cerebral small vessel disease in pseudoxanthoma elasticum: Three cases. *Can. J. Neurol. Sci*. 2005;32:115-118

151. Vahedi K, Massin P, Guichard JP, Miocque S, Polivka M, Goutieres F, Dress D, Chapon F, Ruchoux MM, Riant F, Joutel A, Gaudric A, Bousser MG, Tournier-Lasserve E. Hereditary infantile hemiparesis, retinal arteriolar tortuosity, and leukoencephalopathy. *Neurology,* 2003;60:57-63

152. Verreault S, Joutel A, Riant F, Neves G, Rui Silva M, Maciazek J, Tournier-Lasserve E, Bousser MG, Chabriat H. A novel hereditary small vessel disease of the brain. *Ann. Neurol.* 2006;59:353-357

153. Low WC, Junna M, Borjesson-Hanson A, Morris CM, Moss TH, Stevens DL, St Clair D, Mizuno T, Zhang WW, Mykkanen K, Wahlstrom J, Andersen O, Kalimo H, Viitanen M, Kalaria RN. Hereditary multi-infarct dementia of the swedish type is a novel disorder different from NOTCH3 causing CADASIL. *Brain*. 2007;130:357-367

154. Sourander P, Walinder J. Hereditary multi-infarct dementia. Morphological and clinical studies of a new disease. *Acta Neuropathol*. 1977;39:247-254

155. Colmant HJ, Hagel C, Makrigeorgi-Butera M, Stavrou D. Neuropathology of hereditary subcortical angiopathic encephalopathy. *Clin. Neuropathol*. 2000;19:254-255

156. Hagel C, Groden C, Niemeyer R, Stavrou D, Colmant HJ. Subcortical angiopathic encephalopathy in a german kindred suggests an autosomal dominant disorder distinct from CADASIL. *Acta Neuropathol*. 2004;108:231-240

157. Gunda B, Herve D, Godin O, Bruno M, Reyes S, Alili N, Opherk C, Jouvent E, During M, Bousser MG, Dichgans M, Chabriat H. Effects of gender on the phenotype of CADASIL. *Stroke,* 2012;43:137-141

158. Lipton RB, Bigal ME. The epidemiology of migraine. *Am. J. Med.* 2005;118 Suppl 1:3S-10S

159. Russell MB, Rasmussen BK, Thorvaldsen P, Olesen J. Prevalence and sex-ratio of the subtypes of migraine. *Int. J. Epidemiol*. 1995;24:612-618

160. Russell MB, Rasmussen BK, Fenger K, Olesen J. Migraine without aura and migraine with aura are distinct clinical entities: A study of four hundred and eighty-four male and female migraineurs from the general population. *Cephalalgia,* 1996;16:239-245

161. Bank J, Marton S. Hungarian migraine epidemiology. *Headache,* 2000;40:164-169
162. Brandes JL. The influence of estrogen on migraine: A systematic review. *J. Am. Med. Assoc*. 2006;295:1824-1830
163. Appelros P, Stegmayr B, Terent A. Sex differences in stroke epidemiology: A systematic review. *Stroke,* 2009;40:1082-1090
164. Leys D, Pasquier F, Parnetti L. Epidemiology of vascular dementia. *Haemostasis,* 1998;28:134-150
165. Andersen K, Launer LJ, Dewey ME, Letenneur L, Ott A, Copeland JR, Dartigues JF, Kragh-Sorensen P, Baldereschi M, Brayne C, Lobo A, Martinez-Lage JM, Stijnen T, Hofman A. Gender differences in the incidence of ad and vascular dementia: The EURODEM studies. EURODEM incidence research group. *Neurology,* 1999;53:1992-1997
166. Martin VT, Behbehani M. Ovarian hormones and migraine headache: Understanding mechanisms and pathogenesis--part i. *Headache,* 2006;46:3-23
167. Eikermann-Haerter K, Dilekoz E, Kudo C, Savitz SI, Waeber C, Baum MJ, Ferrari MD, van den Maagdenberg AM, Moskowitz MA, Ayata C. Genetic and hormonal factors modulate spreading depression and transient hemiparesis in mouse models of familial hemiplegic migraine type 1. *J. Clin. Invest.* 2009;119:99-109
168. Krause DN, Duckles SP, Pelligrino DA. Influence of sex steroid hormones on cerebrovascular function. *J. Appl. Physiol*. 2006;101:1252-1261
169. Murphy SJ, McCullough LD, Smith JM. Stroke in the female: Role of biological sex and estrogen. *ILAR journal,* 2004;45:147-159
170. Opherk C, Peters N, Herzog J, Luedtke R, Dichgans M. Long-term prognosis and causes of death in CADASIL: A retrospective study in 411 patients. *Brain,* 2004;127:2533-2539
171. Kin T, Hirano M, Taoka T, Furiya Y, Kataoka H, Kichikawa K, Ueno S. Global and region-specific analyses of apparent diffusion coefficient in dentatorubral-pallidoluysian atrophy. *Am. J. Neuroradiol.* 2006;27:1463-1466
172. Nusbaum AO, Tang CY, Buchsbaum MS, Wei TC, Atlas SW. Regional and global changes in cerebral diffusion with normal aging. *Am. J. Neuroradiol.* 2001;22:136-142
173. Rovaris M, Bozzali M, Iannucci G, Ghezzi A, Caputo D, Montanari E, Bertolotto A, Bergamaschi R, Capra R, Mancardi GL, Martinelli V, Comi G, Filippi M. Assessment of normal-appearing white and gray matter in patients with primary progressive

multiple sclerosis: A diffusion-tensor magnetic resonance imaging study. *Arch. Neurol.* 2002;59:1406-1412

174. Tessa C, Giannelli M, Della Nave R, Lucetti C, Berti C, Ginestroni A, Bonuccelli U, Mascalchi M. A whole-brain analysis in de novo Parkinson disease. *Am. J. Neuroradiol.* 2008;29:674-680

175. Vrenken H, Pouwels PJ, Geurts JJ, Knol DL, Polman CH, Barkhof F, Castelijns JA. Altered diffusion tensor in multiple sclerosis normal-appearing brain tissue: Cortical diffusion changes seem related to clinical deterioration. *J. Magn. Reson. Imaging*. 2006;23:628-636

176. Chua TC, Wen W, Slavin MJ, Sachdev PS. Diffusion tensor imaging in mild cognitive impairment and Alzheimer's disease: A review. *Curr. Opin. Neurol,* 2008;21:83-92

177. Mascalchi M, Tessa C, Moretti M, Della Nave R, Boddi V, Martini S, Inzitari D, Villari N. Whole brain apparent diffusion coefficient histogram: A new tool for evaluation of leukoaraiosis. *J. Magn. Reson. Imaging*. 2002;15:144-148

178. Nitkunan A, Charlton RA, McIntyre DJ, Barrick TR, Howe FA, Markus HS. Diffusion tensor imaging and mr spectroscopy in hypertension and presumed cerebral small vessel disease. *Magn. Reson. Med*. 2008;59:528-534

179. Nusbaum AO, Tang CY, Wei T, Buchsbaum MS, Atlas SW. Whole-brain diffusion mr histograms differ between ms subtypes. *Neurology*, 2000;54:1421-1427

180. O'Sullivan M, Singhal S, Charlton R, Markus HS. Diffusion tensor imaging of thalamus correlates with cognition in CADASIL without dementia. *Neurology*, 2004;62:702-707

181. Schmidt R, Ropele S, Ferro J, Madureira S, Verdelho A, Petrovic K, Gouw A, van der Flier WM, Enzinger C, Pantoni L, Inzitari D, Erkinjuntti T, Scheltens P, Wahlund LO, Waldemar G, Rostrup E, Wallin A, Barkhof F, Fazekas F. Diffusion-weighted imaging and cognition in the leukoariosis and disability in the elderly study. *Stroke,* 41:e402-408

182. Chabriat H. Diffusion histograms in CADASIL. *Stroke*, 2005;36:2526

183. Cercignani M, Bammer R, Sormani MP, Fazekas F, Filippi M. Inter-sequence and inter-imaging unit variability of diffusion tensor MR imaging histogram-derived metrics of the brain in healthy volunteers. *Am. J. Neuroradiol.* 2003;24:638-643

184. Steens SC, Admiraal-Behloul F, Schaap JA, Hoogenraad FG, Wheeler-Kingshott CA, le Cessie S, Tofts PS, van Buchem MA. Reproducibility of brain ADC histograms. *Eur. Rradiol*. 2004;14:425-430

185. Viswanathan A, Guichard JP, Gschwendtner A, Buffon F, Cumurcuic R, Boutron C, Vicaut E, Holtmannspotter M, Pachai C, Bousser MG, Dichgans M, Chabriat H. Blood pressure and haemoglobin a1c are associated with microhaemorrhage in CADASIL: A two-centre cohort study. *Brain*, 2006;129:2375-2383

186. Rasmussen BK, Olesen J. Migraine with aura and migraine without aura: An epidemiological study. *Cephalalgia*, 1992;12:221-228; discussion 186

187. MacGregor EA. Oestrogen and attacks of migraine with and without aura. *Lancet Neurol*. 2004;3:354-361

188. Bolay H, Reuter U, Dunn AK, Huang Z, Boas DA, Moskowitz MA. Intrinsic brain activity triggers trigeminal meningeal afferents in a migraine model. *Nature Medicine*, 2002;8:136-142

189. Eikermann-Haerter K, Kudo C, Moskowitz MA. Cortical spreading depression and estrogen. *Headache*, 2007;47 Suppl 2:S79-85

190. Sachs M, Pape HC, Speckmann EJ, Gorji A. The effect of estrogen and progesterone on spreading depression in rat neocortical tissues. *Neurobiology of Disease*. 2007;25:27-34

191. Eikermann-Haerter K, Baum MJ, Ferrari MD, van den Maagdenberg AM, Moskowitz MA, Ayata C. Androgenic suppression of spreading depression in familial hemiplegic migraine type 1 mutant mice. *Ann. Neurol*. 2009;66:564-568

192. Eikermann-Haerter K, Yuzawa I, Dilekoz E, Joutel A, Moskowitz MA, Ayata C. Cerebral autosomal dominant arteriopathy with subcortical infarcts and leukoencephalopathy syndrome mutations increase susceptibility to spreading depression. *Ann. Neurol.* 69:413-418

193. Reeves MJ, Bushnell CD, Howard G, Gargano JW, Duncan PW, Lynch G, Khatiwoda A, Lisabeth L. Sex differences in stroke: Epidemiology, clinical presentation, medical care, and outcomes. *Lancet Neurol*. 2008;7:915-926

194. McCullough LD, Alkayed NJ, Traystman RJ, Williams MJ, Hurn PD. Postischemic estrogen reduces hypoperfusion and secondary ischemia after experimental stroke. *Stroke,* 2001;32:796-802

195. McCullough LD, Hurn PD. Estrogen and ischemic neuroprotection: An integrated view. *Trends Endocrin. Met*. 2003;14:228-235

196. Wyller TB. Stroke and gender. *J. Gend. Specif. Med*. 1999;2:41-45

197. Reyes S, Viswanathan A, Godin O, Dufouil C, Benisty S, Hernandez K, Kurtz A, Jouvent E, O'Sullivan M, Czernecki V, Bousser MG, Dichgans M, Chabriat H. Apathy: A major symptom in CADASIL. *Neurology*, 2009;72:905-910

198. Jouvent E, Reyes S, Mangin J, Roca P, Perrot M, Thyreau B, Hervé D, Dichgans M, Chabriat H. Apathy is related to cortex morphology in CADASIL: A sulcal-based morphometry study. *Neurology*, 2011

199. Viscoli CM, Brass LM, Kernan WN, Sarrel PM, Suissa S, Horwitz RI. A clinical trial of estrogen-replacement therapy after ischemic Stroke, *The New England journal of medicine*. 2001;345:1243-1249

200. Wassertheil-Smoller S, Hendrix SL, Limacher M, Heiss G, Kooperberg C, Baird A, Kotchen T, Curb JD, Black H, Rossouw JE, Aragaki A, Safford M, Stein E, Laowattana S, Mysiw WJ. Effect of estrogen plus progestin on stroke in postmenopausal women: The women's health initiative: A randomized trial. *J. Am. Med. Assoc*. 2003;289:2673-2684

201. Dichgans M, Putz B, Boos D, Auer DP. Role of subvoxel free fluid on diffusion parameters in brain tissue with cerebral autosomal dominant arteriopathy with subcortical infarcts and leukoencephalopathy and its correlation with physical disability: Histogram analysis of standard and fluid-attenuated mr diffusion. *Am. J. Neuroradiol*. 2003;24:1083-1089

Publications

Gunda B, Várallyay Gy, Rudas G, Bereczki D, Challenges in diagnosing cerebral lacunar infarcts, *Curr. Med. Imaging Rev*. 2009, 5, 75-84.

Gunda B, Chabriat H, Bereczki D. CADASIL and other hereditary small vessel diseases of the brain-increasingly diagnosed conditions underlying familial ischemic stroke and dementia. *Ideggyogy Sz.* 2011 Mar 30; 64 (3-4):88-100.

Gunda B, Hervé D, Godin O, Bruno M, Reyes S, Alili N, Opherk C, Jouvent E, Düring M, Bousser MG, Dichgans M, Chabriat H. Effects of Gender on the Phenotype of CADASIL. *Stroke*, 2012 Jan; 43(1):137-41.

Gunda B, Várallyay Gy, Bereczki D. Multimodal MRI of cerebral small vessel disease. In: Peter Bright (ed.), *Neuroimaging –Clinical Applications*, ISBN 978-953-51-0200-7, InTech, Mar 2012: 277-300.

(All in the topic of the present thesis.)

Acknowledgements

First of all I would like to thank my supervisor professor Dániel Bereczki for his wise and inspiring guidance all through my studies. I am grateful both for his professional and human support in my scientific and clinical work. It is him to whom I owe the most in the making of this thesis.

I am also thankful to my colleagues at the Department of Neurology at Semmelweis University for helping my work wherever possible. I would also like to render thanks to the Head of the MR Research Centre, Gábor Rudas, and all the radiologist colleagues who introduced me into neuroimaging. My special thanks go to György Várallyay –a dedicated, patient and profoundly humane teacher.

This thesis could not have been written without my fortunate stay at the centre of rare cerebrovascular diseases (CERVCO) at Hôpital Lariboisière in Paris-an outstanding workshop of clinical neurology organised by Marie-Germaine Bousser and currently led by Hugues Chabriat. I am grateful to him and his team who were exceedingly helpful, friendly and open towards me. Their work as a clinical and scientific team was exemplary to me. The scientific thinking, critical attitude and methodology that I learned from Professor Chabriat will accompany me in my whole professional career.

My work was financially supported by grants from the European Federation of Neurological Societies (EFNS) and Institut Servier in Paris and the Hungarian Government at my home institution (TÁMOP).

Finally and most of all I am thankful to my Family. Primarily to my Wife, Dóra Gunda-Szabó, who encouraged, accompanied, tolerated me and gave up her ways for mine. To my Parents who provided everything I needed to pursue my ambitions. Finally to my Daughter, Julka, who just happened to appear along the way and is a source of unprecedented happiness.